The Abdus Salam
International Centre for Theoretical Physics

United Nations
Educational, Scientific and
Cultural Organization

IAEA
International Atomic Energy Agency

1932-17

Winter College on Micro and Nano Photonics for Life Sciences

11 - 22 February 2008

Scanning IR-nearfield optical microscopy (SNIM)

Martina Havenith
Ruhr University Bochum
Bochum, Germany

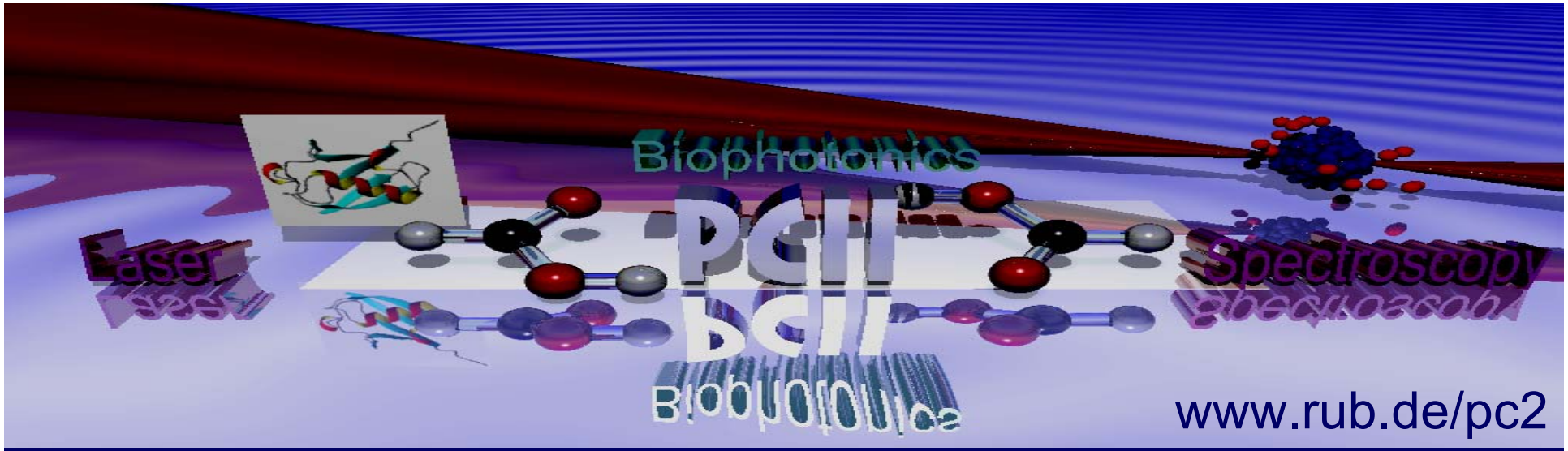

IR-nearfield microscopy

M. Havenith

Physical Chemistry, Ruhr-Universität Bochum, Germany

Münster, 17.12.07

Taking a closer look on surfaces and interfaces: Spectral Fingerprints

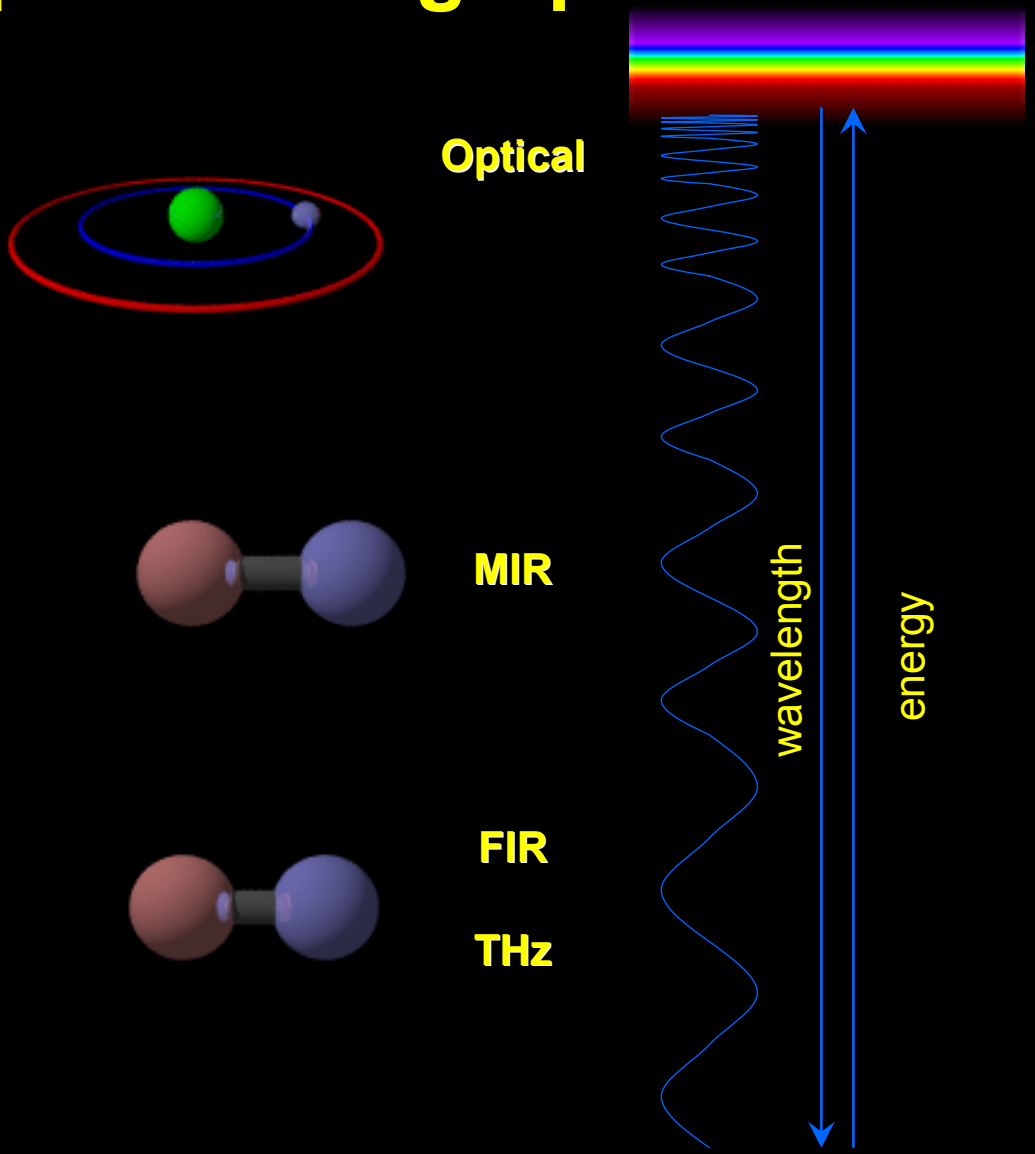

Skeleton motions
Breathing modes
Large amplitude vibrations

Intermolecular modes
Phonons

Determination of structure

Biology: a “physicist” view

Cytosol: High concentration of Protein (1650 cm^{-1} Amid I band)

Membrane: Strong absorption of lipids at 2920 cm^{-1}

Nucleus with **DNA** in high concentration: Strong absorption at 1240 cm^{-1}

Water: percentage of water 60-98%: high absorption coefficient in the IR and NIR

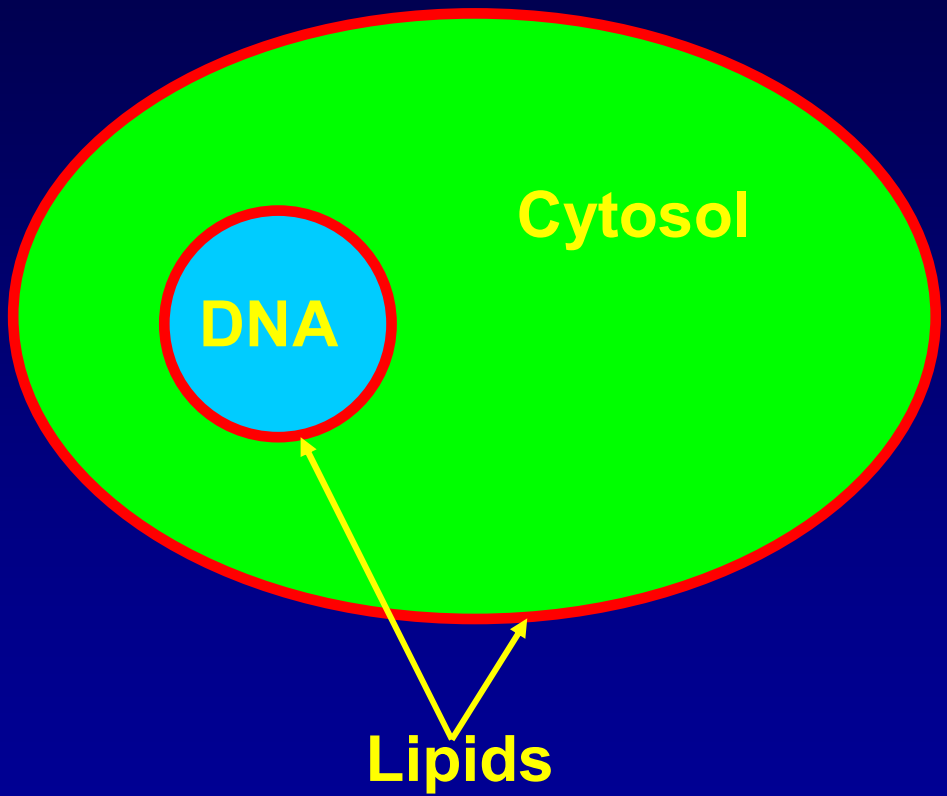

Fingerprint region of infrared vibration bands

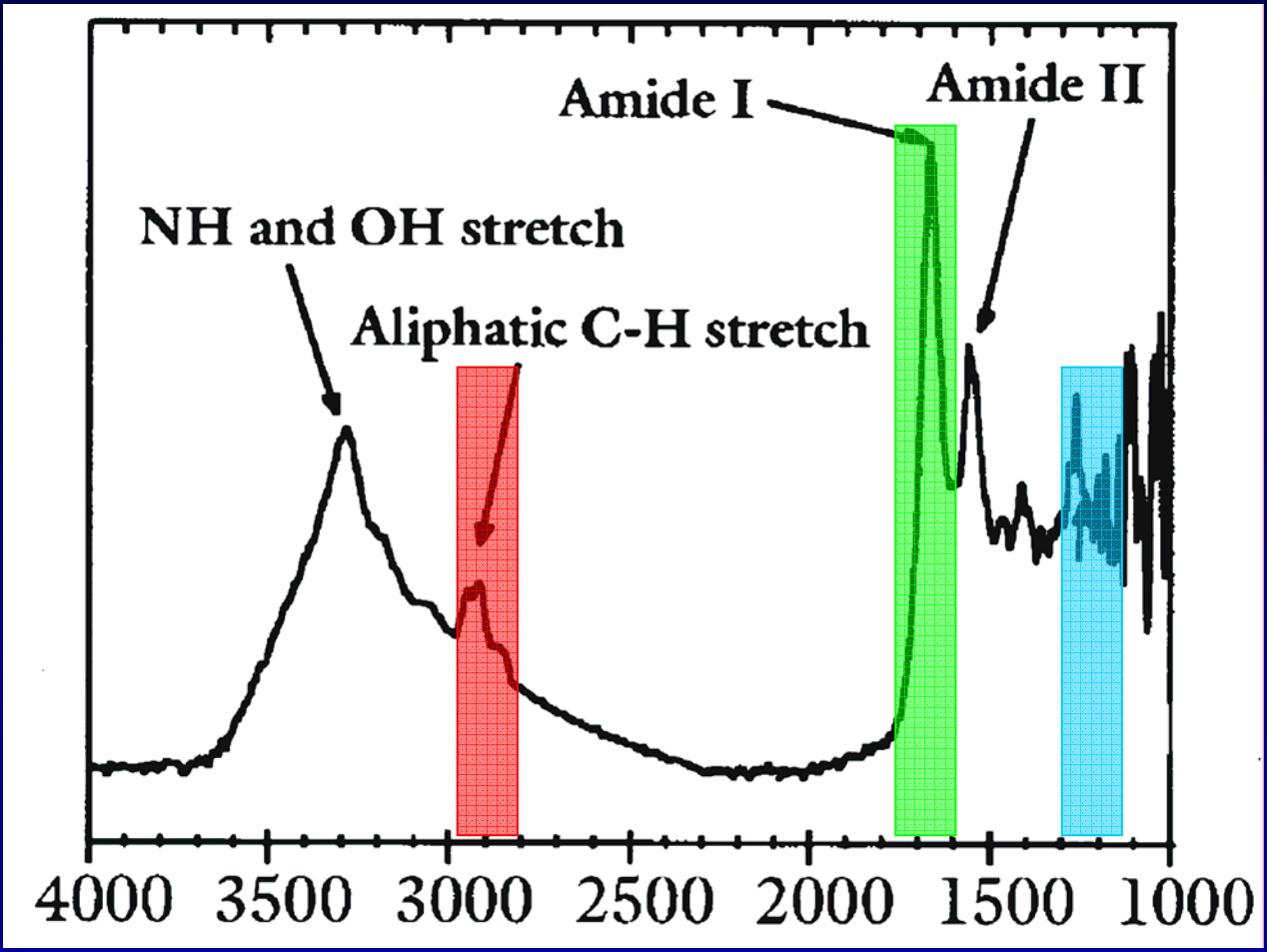

A cheap chemical microscope

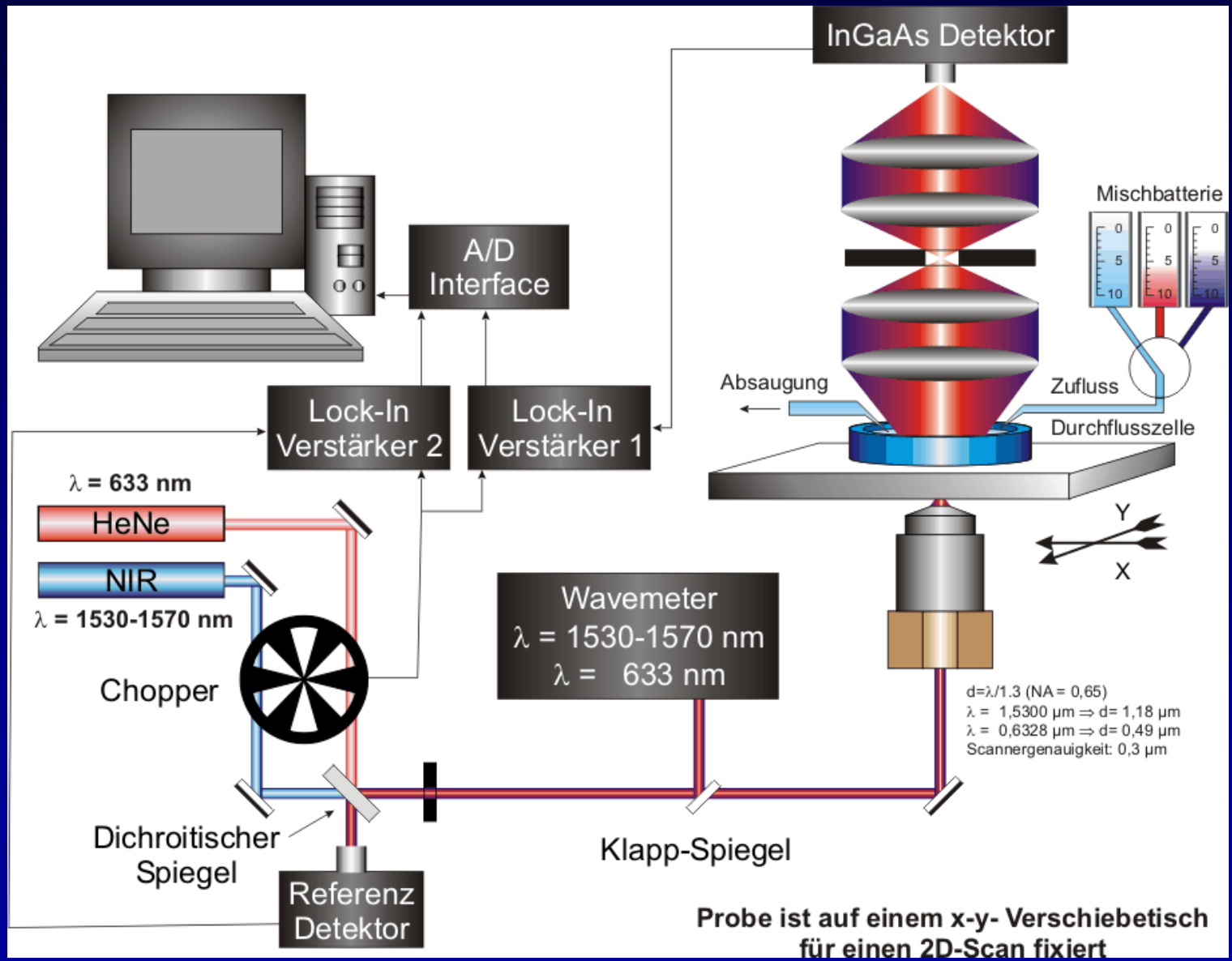

Measurement of intracellular water

- Intracellular water concentration is important for cell function
- Hormone, Oxidative stress, miniomla dosis of pharmaceuticals can alter the intracellular water concentration
- Change of osmotic pressure causes cell swelling or cell shrinkage
- Intracellular water concentration influences protein syntheses, cell proliferation, cell death (apotheosis)
- **Dream of medicine: control of intracellular water concentration**

Influence of minimum dosages of pharmaceuticals on single cell

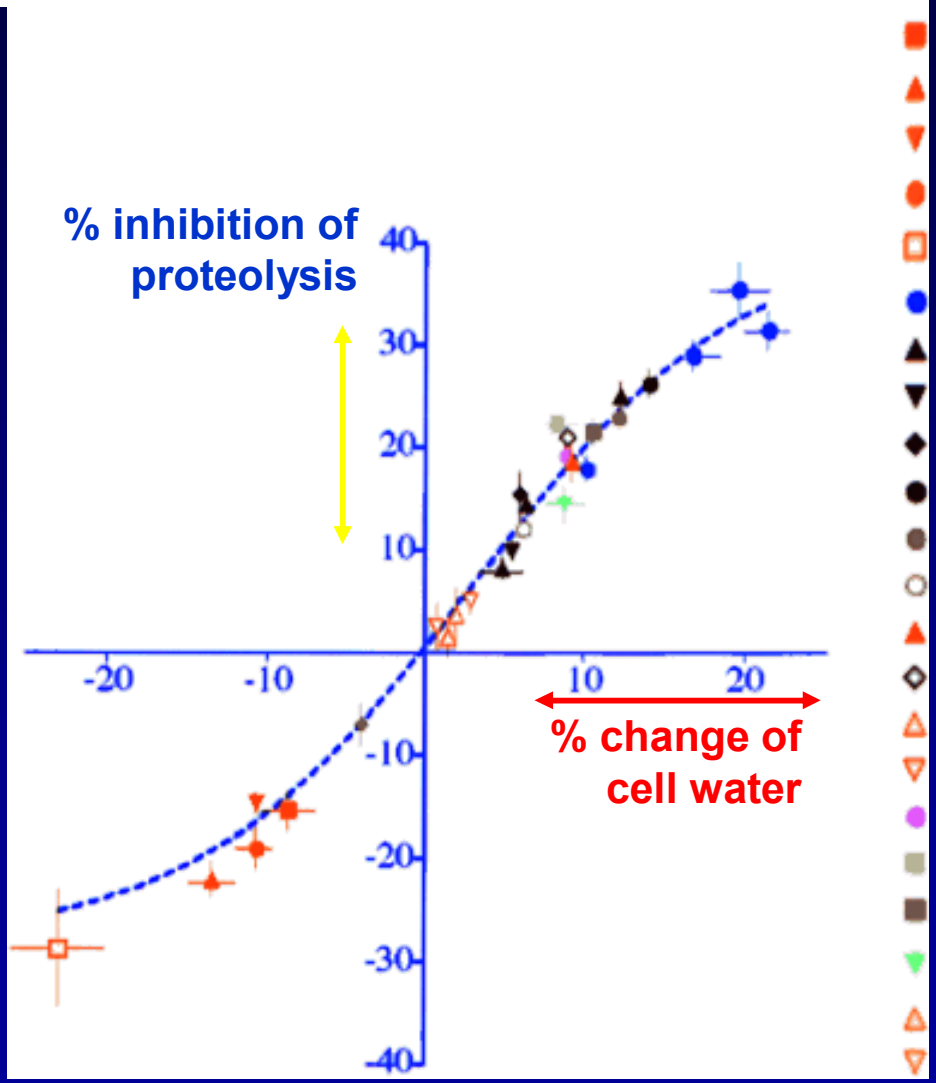

- Insulin + cAMP
- cAMP/Hypoosmolarity
- Glucagon/Hypoosmolarity
- Glucagon/Insulin
- Hyperosmolarity/Insulin
- cAMP + Vasopressin
- Hypoosmolarity
- Glutamine
- Glycine
- Alanine
- Glutamine + Glycine
- Insulin
- Insulin/Bumetanide
- Ethanol
- Acetaldehyde
- Ethanol/Bumetanide
- Ethanol/Methylpyrazol
- Taurocholate
- Glycerol
- IGF1
- $BaCl_2$
- Glucagon + Hypoosmolarity
- Glucagon + Insulin

Liver Cell Hydration and Proteolysis

Study of Prof. Häussinger (medicine)

A non-invasive method to quantify water in living cells

- **Water:** most abundant substance in organisms
- Chemical reactions of all organism take place in aqueous solution
- Transport of solutes
- Temperature regulation
- NIR overtone transition ($\Delta v=2$), weaker than $\Delta v=1$ Absorption, but still penetrating

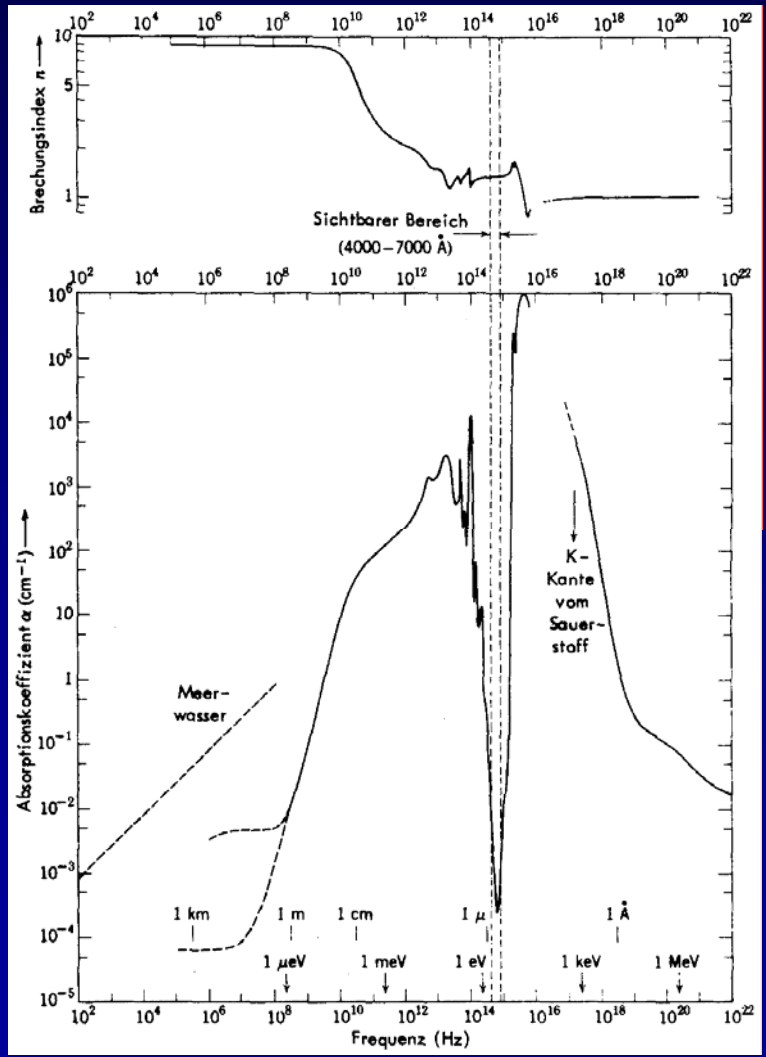

Experimental Results:

Swelling: volume increases by a factor of 3
Intracellular water concentration:
first increase (dilution), followed by a decrease
Explanation:
Onset of protein synthesis yields a decrease
in relative water concentration

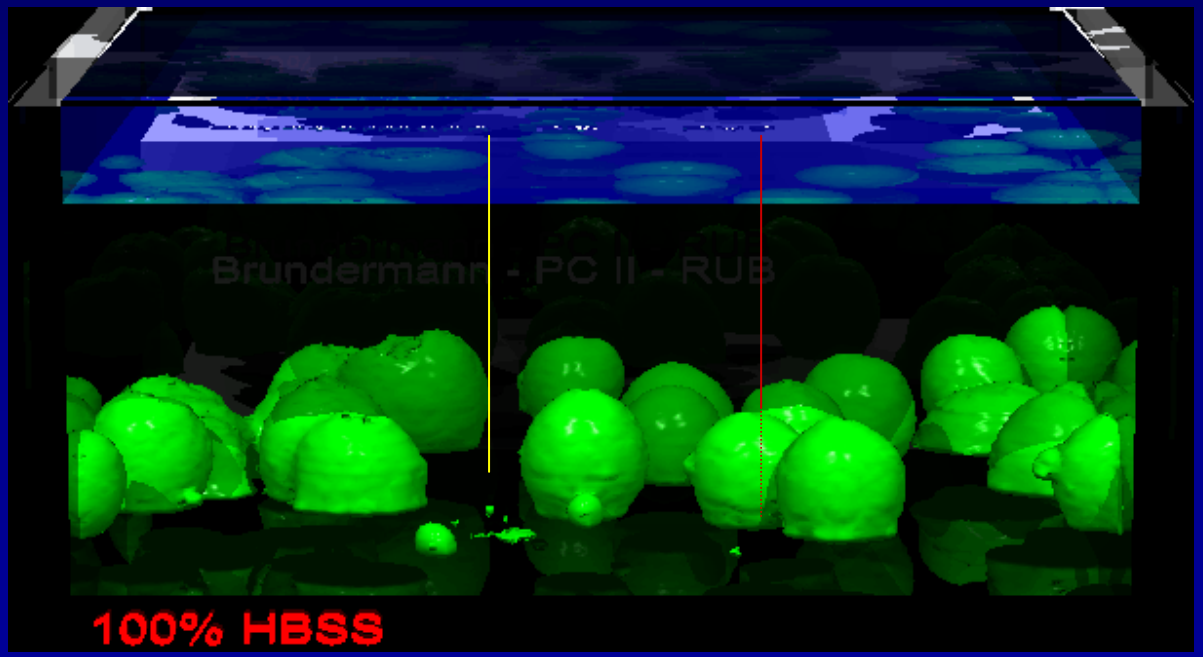

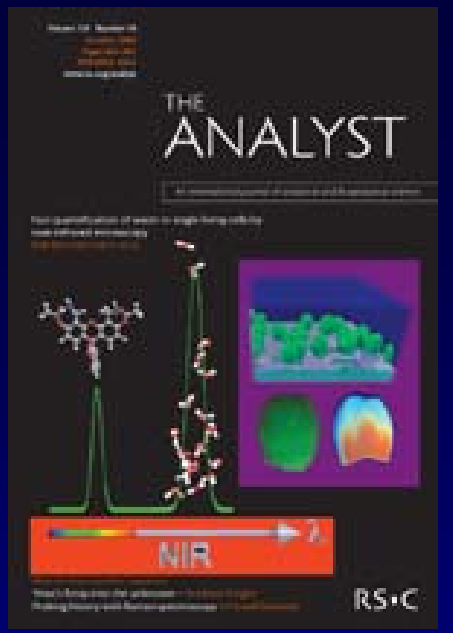

$I(v) = I_0 \exp(-\alpha(v)l)$

reference:
absorption by HBSS

absorption by intra-cellular water + HBSS

E. Bründermann, E. Bründermann, A. Bergner, F. Petrat, R. Schiwon, G. Wollny, I. Kopf, H. de Groot, M. Havenith, Analyst, 129, 893 (2004)

Future potential for medical applications: Monitoring the influence of pharmaceuticals on a single cell level in real time

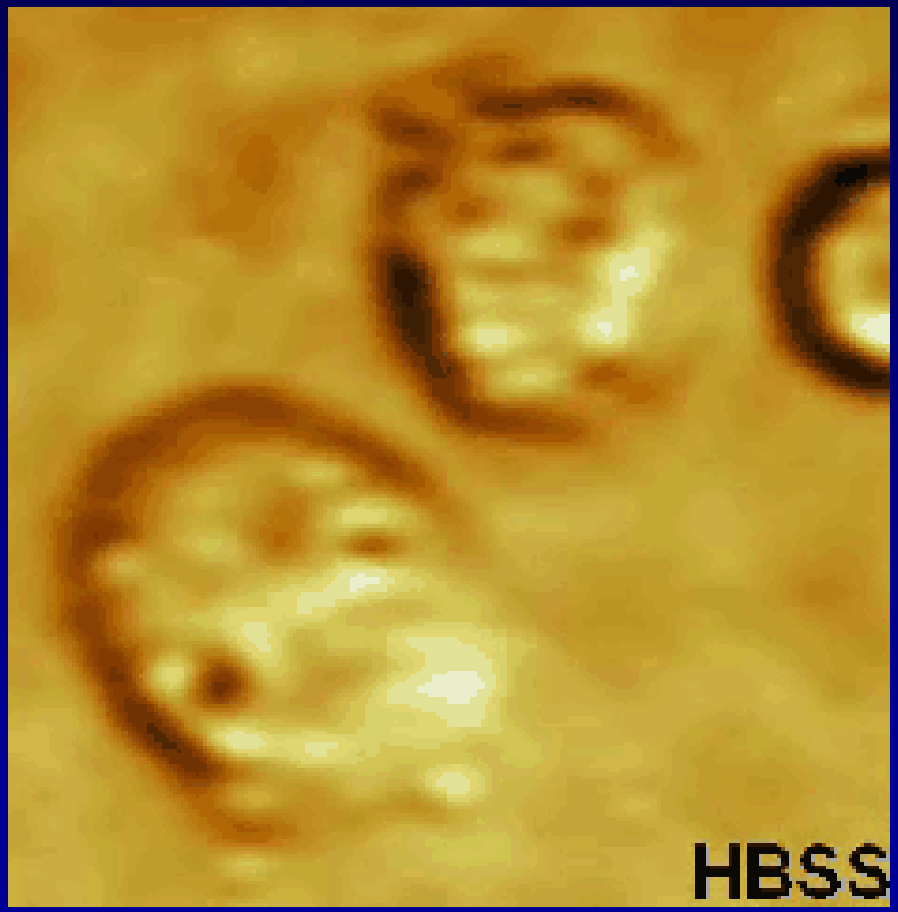

Chemical Science

Research highlights

by the Royal Society, November 2004

Tracking drugs in single cells

„A non-invasive method
To quantify water in living
cells is being pioneerd in Germany“

Future improvements:

Tomography

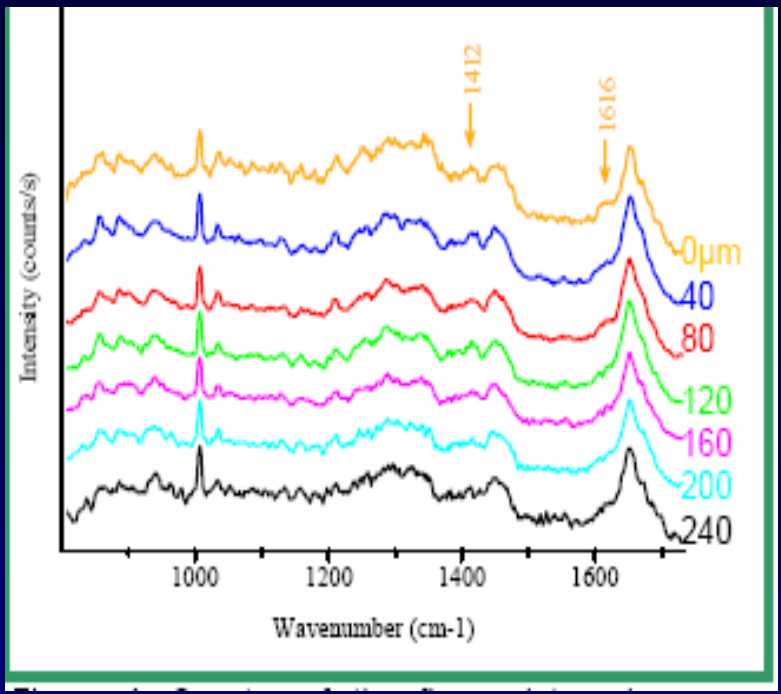

Confocal Raman microscopy of human skin (WITEC)

Peak Position (cm^{-1})	Protein Assignments	Lipid Assignments	Others
1745		V(C=0)	
1655	V(C=0)Amide I		
1445	$\delta(CH_2)$, $\delta(CH_3)$ δ	$\delta(CH_2)$ scissoring	
1301		$\delta(CH_2)$ twisting, wagging	
1269	v(CN), δ(NH) Amide III		
1080		v(CC)skeletal	v(CC), $v_s(PO_2)$
1030		v(CC) skeletal	Nucleic acids
1002	v(CC) Phenyl ring		
938	v(CC) praline, valine		
855	δ(CCH) aromatic, olefinic		polysaccaride
822	δ(CCH) aliphatic		

Table 1: Summary of major vibrational bands identified in skin: v, stretching mode; v_s, symmetric stretch; δ, bending mode.

3/5

Spectral fingerprints

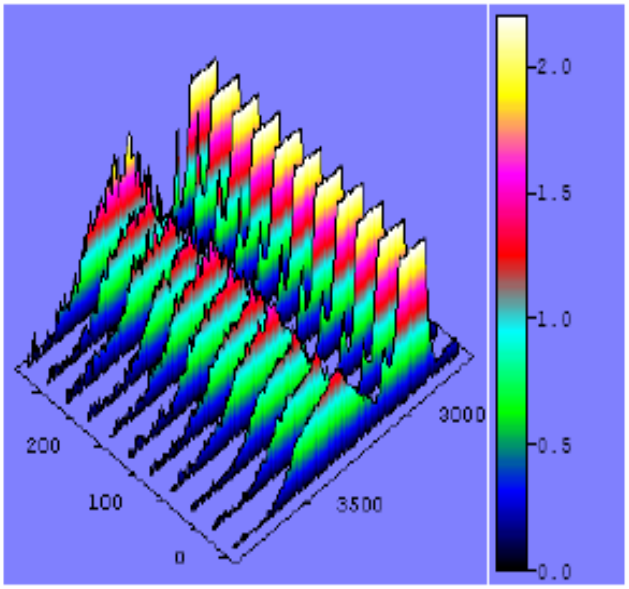

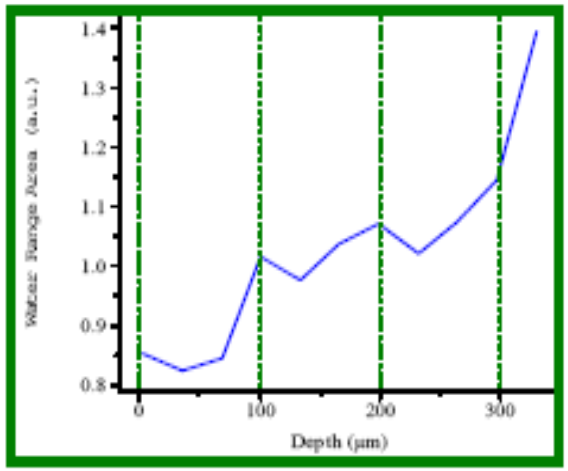

Figure 5 : Non hydrated skin (a) 3D view of the spectra of the CH/OH region recorded at different depths within the non hydrated skin. (b) In-depth profile of the relative evolution of the ν(OH) band area [3350-3550]cm^{-1}.

measurement of hydration in human skin

hydration in dependence of depth

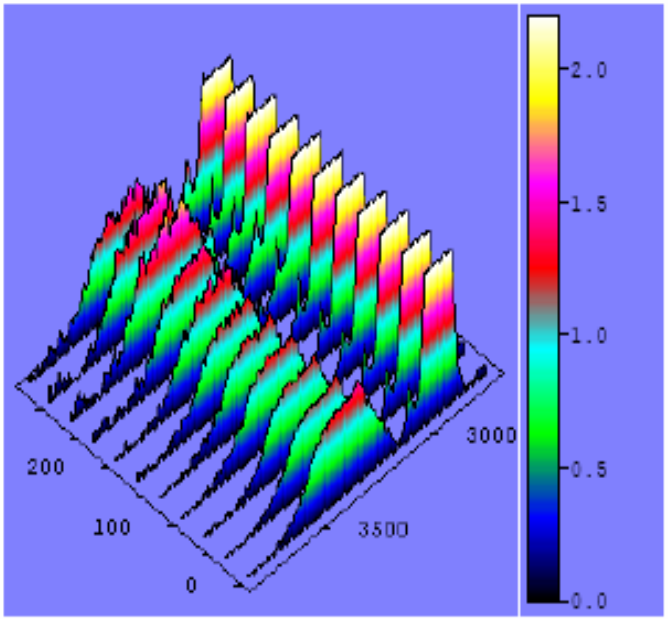

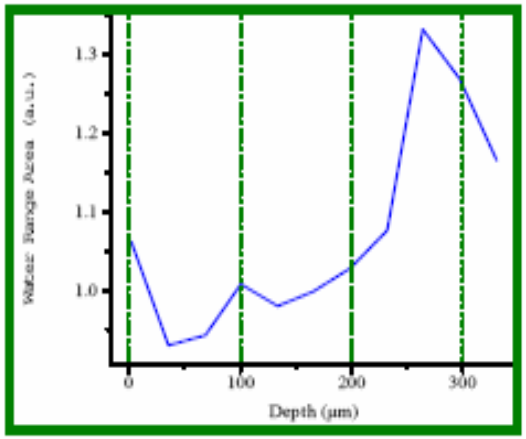

Figure 6 : Hydrated skin (a) 3D view of the spectra of the CH/OH region recorded at different depths within the hydrated skin. (b) In-depth profile of the relative evolution of the ν(OH) band area [3350-3550]cm^{-1}.

„Chemical Microscopy“ in the IR-and THz : advantage: Marker free disadvantage: diffraction limited

SENTERRA Raman Microscope

Abbe Limit: lateral resolution > λ/2

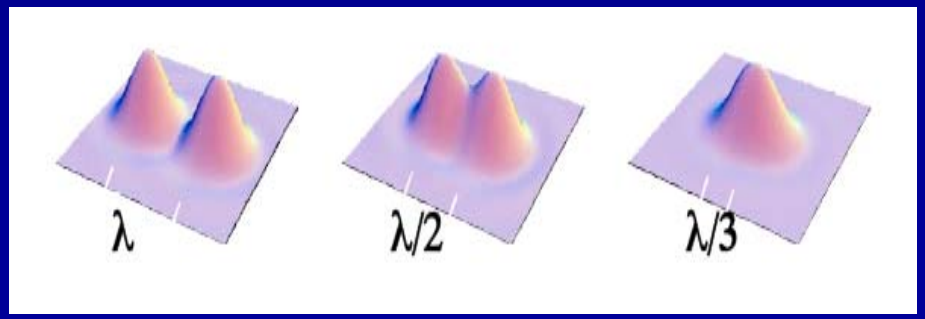

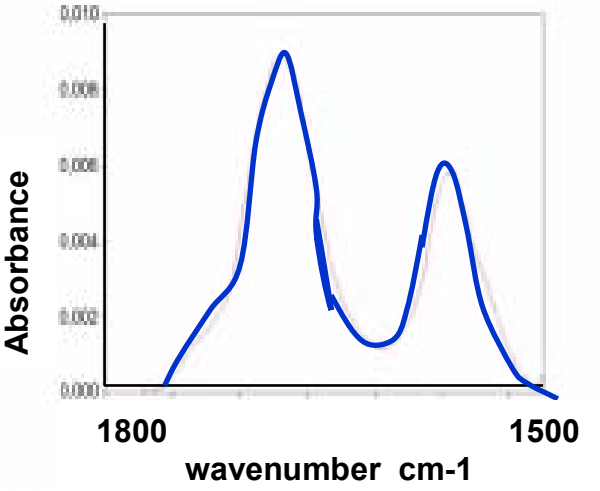

Figure 2

Figure 2: Absorption spectrum of an ultrathin protein layer on a gold coated substrate. The shape of the amide bands at ~1540cm^{-1} and 1670cm^{-1} can give valuable information about the conformation of the protein molecules.

Senterra Raman microscope

Atomic force field microscopy (AFM)
measurement of topography
nm lateral resolution

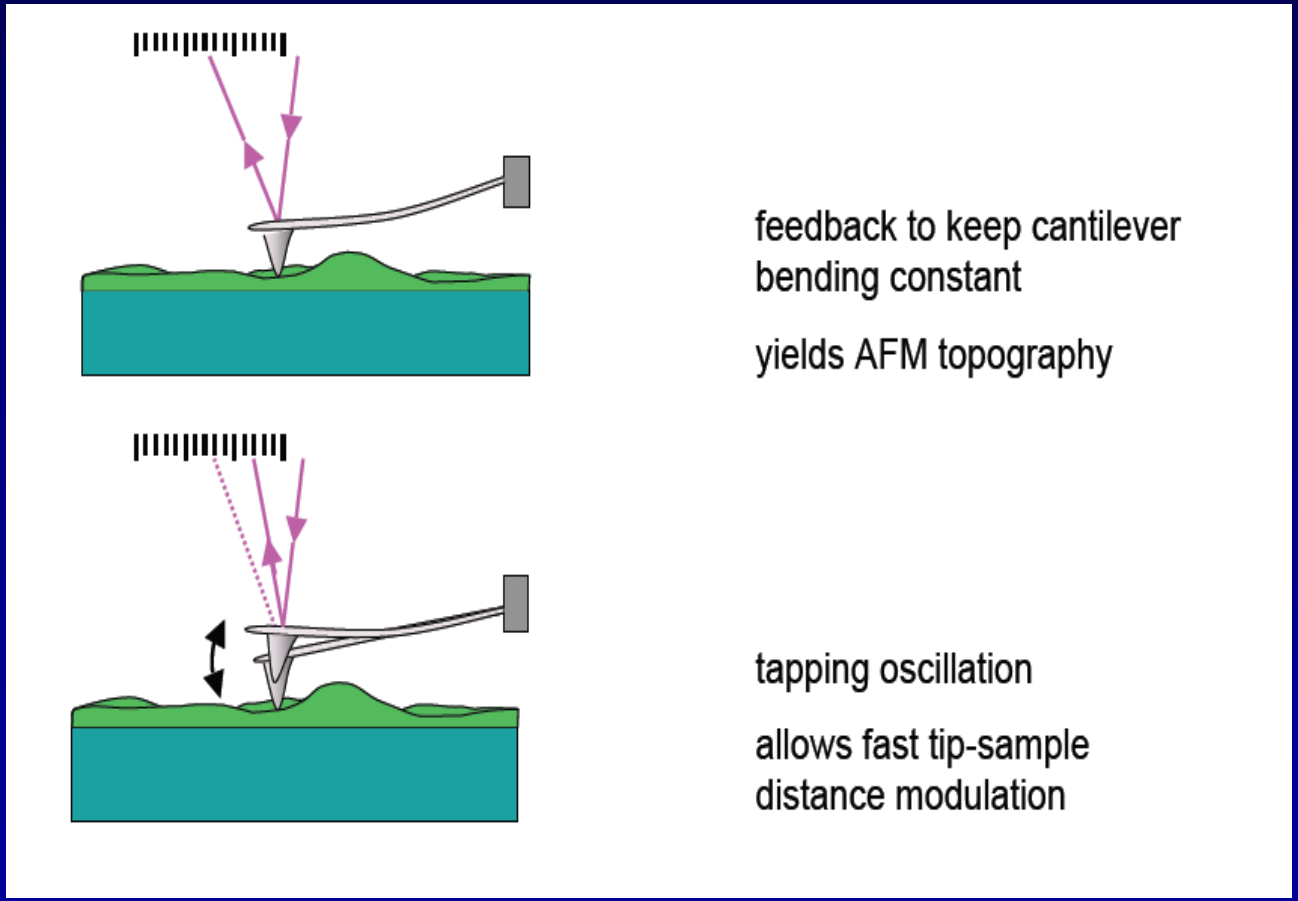

1986:
G. Binning, C. Quate, Ch. Gerber

Infrared Near field microscopy
Chemical imaging beyond the wave length limit

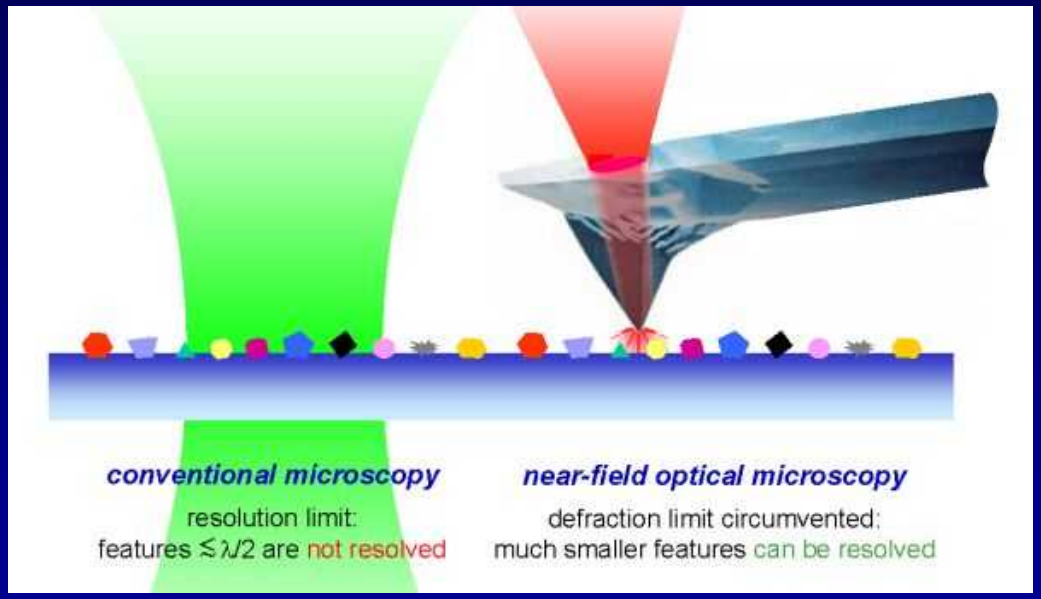

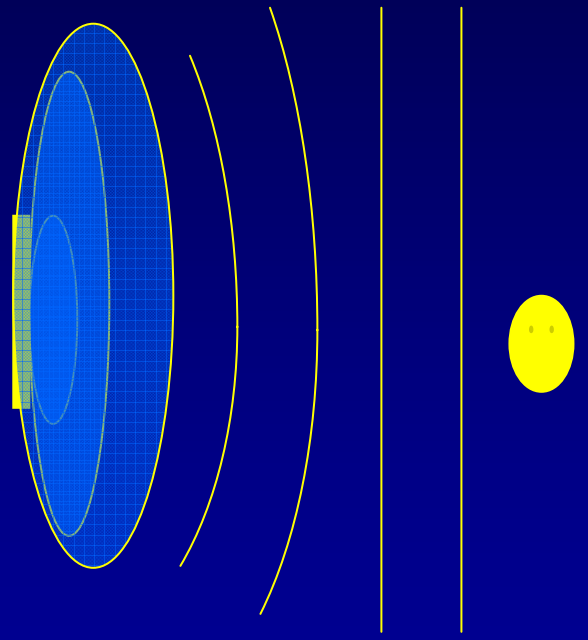

Far field
Plane wave

Infrared Near field microscopy
Chemical imaging beyond the wave length limit

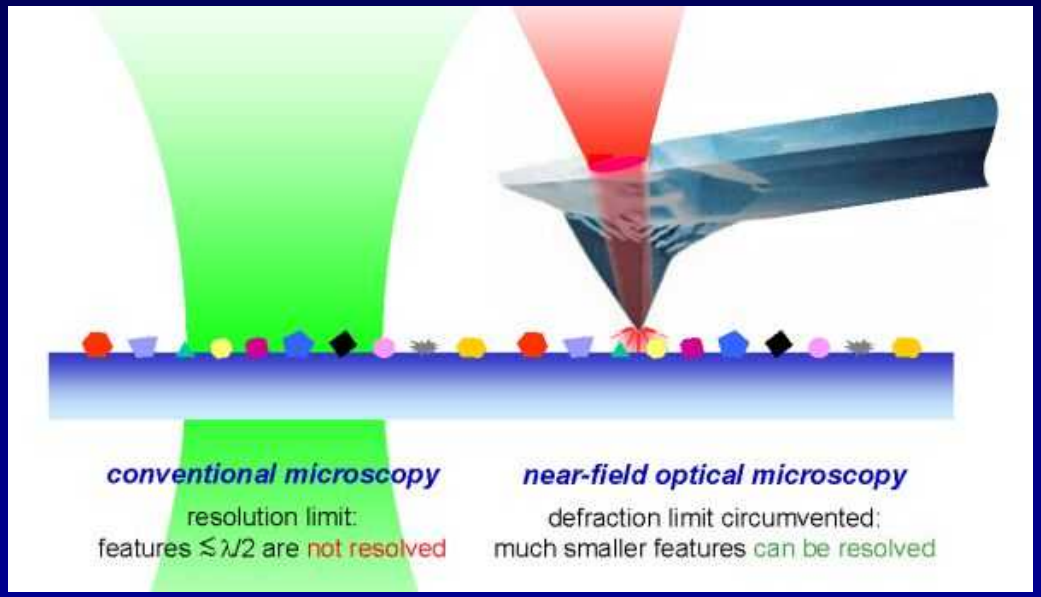

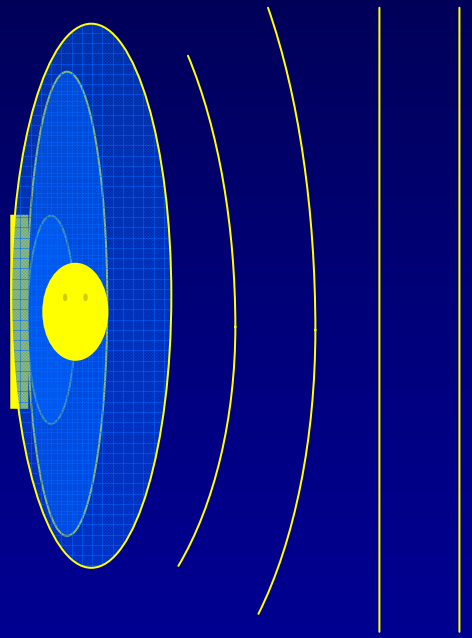

Near field

Infrared Near field microscopy
Chemical imaging beyond the wave length limit

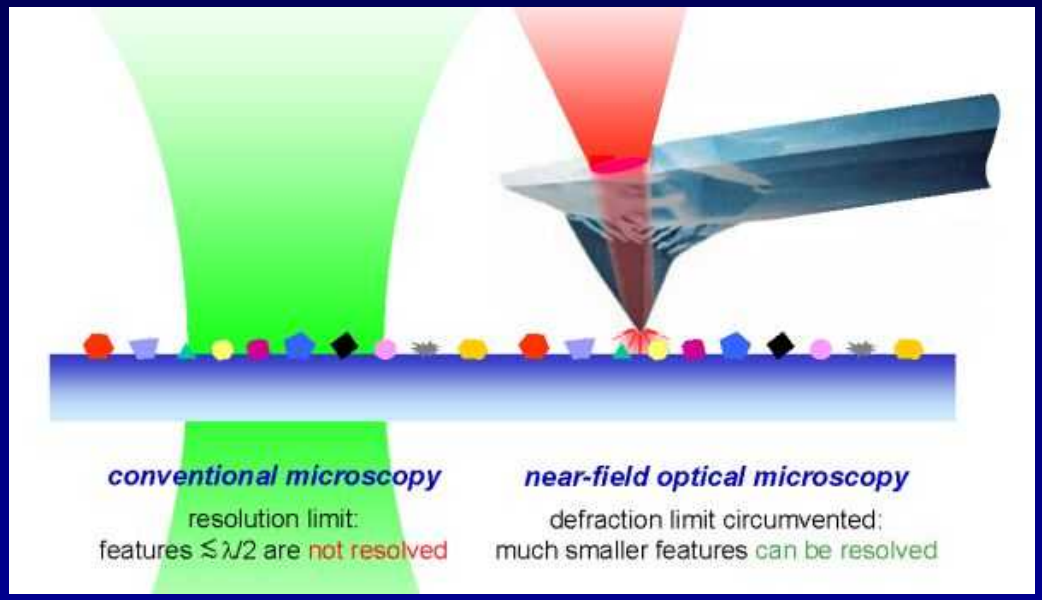

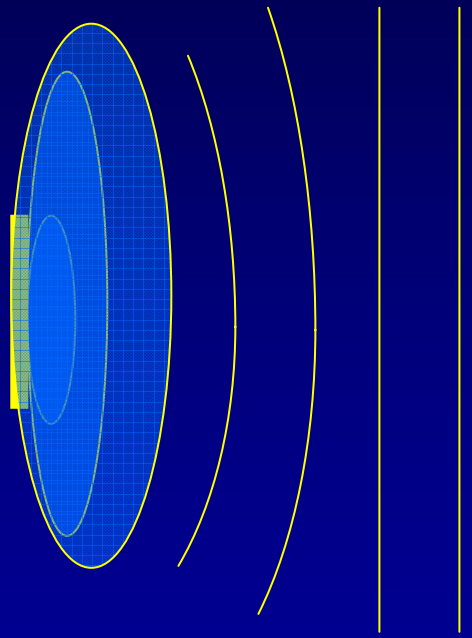

Nano aperature

Nano antenna

Near field microscopy
Microscopy beyond the wave length limit

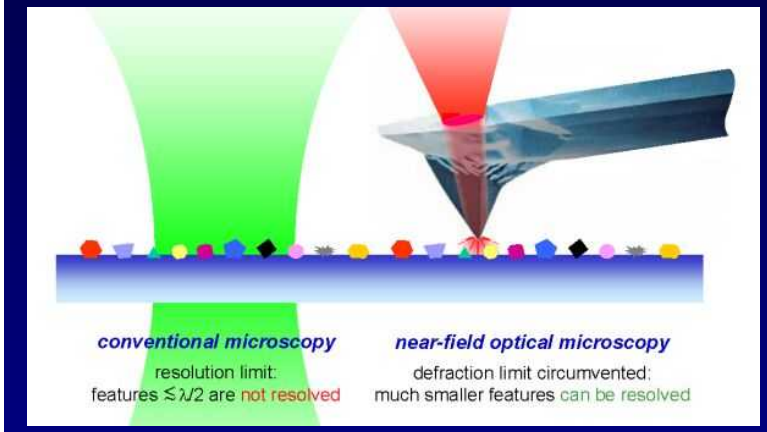

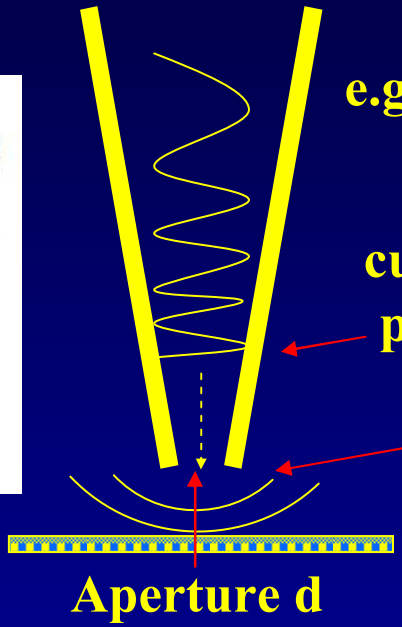

e.g. glass fiber coated with metal

cut-off point $\lambda/2$

evanescent field with exponential decay

z max. 0.1·d

Aperture d

VIS	angle : 10 - 20° d : 100 - 50 nm	→	10^{-3} - 10^{-6} transmission
IR	d : 100 nm	→	10^{-25} transmission

High power IR-radiation
IR-cw Opto Parametric Oscillator (2.9 W)

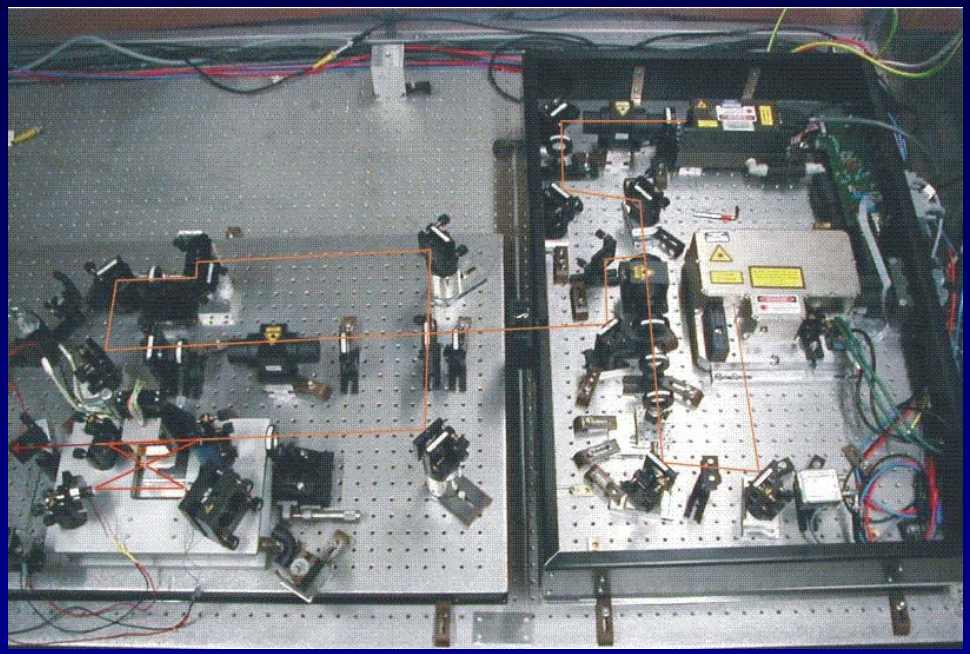

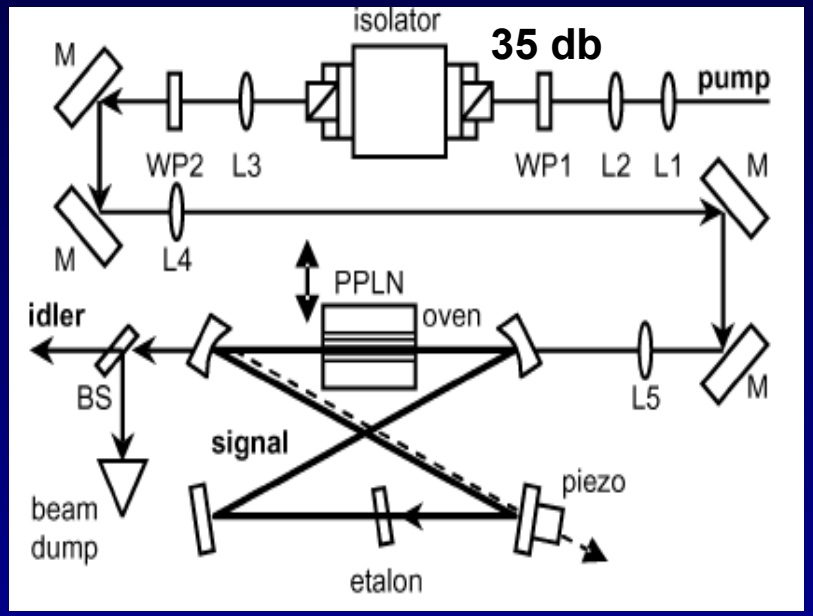

Pump laser: **M**aster **O**scillator **P**ower **A**mplifier: output power: 20 W at 1064 nm
Periodically **P**oled **L**ithium **N**iobate (quasiphase matched) 19 poling areas
end caps are tilted to prevent back reflection; tripe band antireflection coating
cw IR radiation 2.9 W
resonant for signal wavelength (1485-1.665 nm) ; idler (3000-4000 nm)
Faraday isolator; three lens system for proper phase matching

Apertureless near-field using our high power IR-cw OPO (2.9 W) !

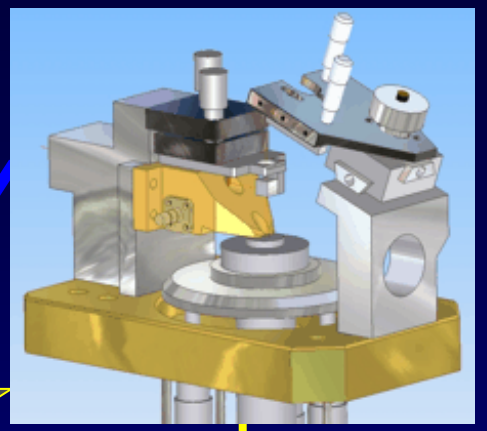

[1] Knoll, B. and Keilmann, F.*"Near-field probing of vibrational absorption for chemical microscopy"* Nature **399** 134-137 (1999)
[2] A. Lahrech, R. Bachelot, P. Gleyzes, A.C. Boccara, *"Infrared-reflection-mode near-field microscopy using an apertureless probe with a resolution of λ/600", Optics Letters* **21**, 1315-1317 (1996).

A chemical nanoscope: contrast mechanism

dipole

$$p_p = \alpha_p \left(E_{inc} + E_s\right)$$
$$p_s = \alpha_s \left(E_{inc} + E_p\right)$$

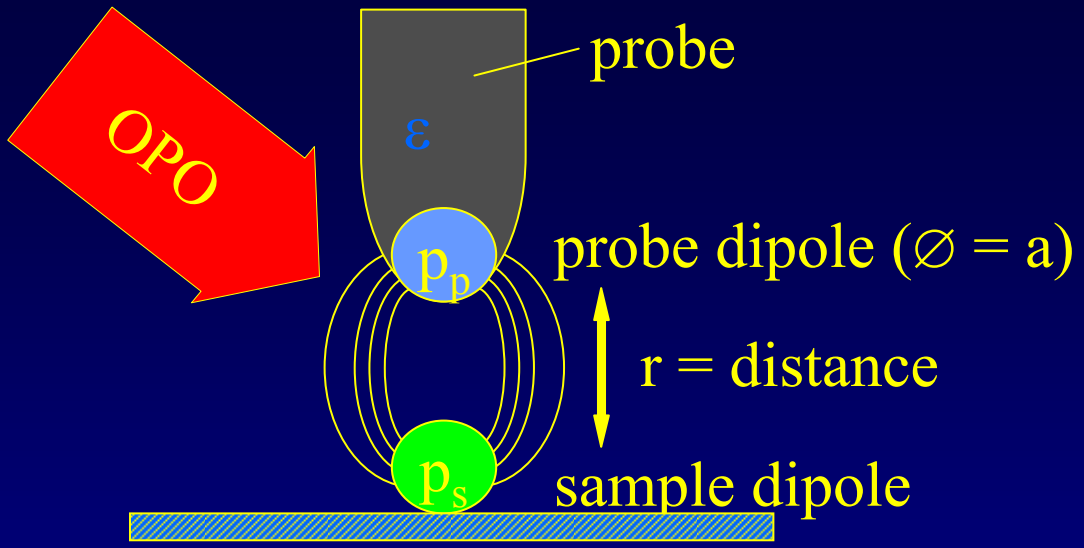

p-polarization

$$\alpha^{eff} = \frac{\alpha_p + \alpha_s + \frac{\alpha_p \alpha_s}{\pi} \cdot \frac{1}{r^3}}{1 - \frac{\alpha_p \alpha_s}{4\pi^2} \cdot \frac{1}{r^6}}$$

s-polarization

$$\alpha^{eff} = \frac{\alpha_p + \alpha_s - \frac{\alpha_p \alpha_s}{\pi} \cdot \frac{1}{r^3}}{1 - \frac{\alpha_p \alpha_s}{16\pi^2} \cdot \frac{1}{r^6}}$$

- r >> a, sum of the polarizabilities
- otherwise, dipole-dipole interaction
- p-polarization : increase
- s-polarization : decrease

} of $\alpha \propto E_{sca}$

- $\sigma_{scatt} \propto k^4 |\alpha^{eff}|^2$
- absorption $\propto$ Im (α^{eff})

Scanning near-field infrared microscopy (SNIM)
Chemical fingerprints beyond the diffraction limit

(λ = 3,22 μm; ν = 3100 cm^{-1})

30 nm gold balls on glas

physical nanoscope

topography

chemical nanoscope

Near field

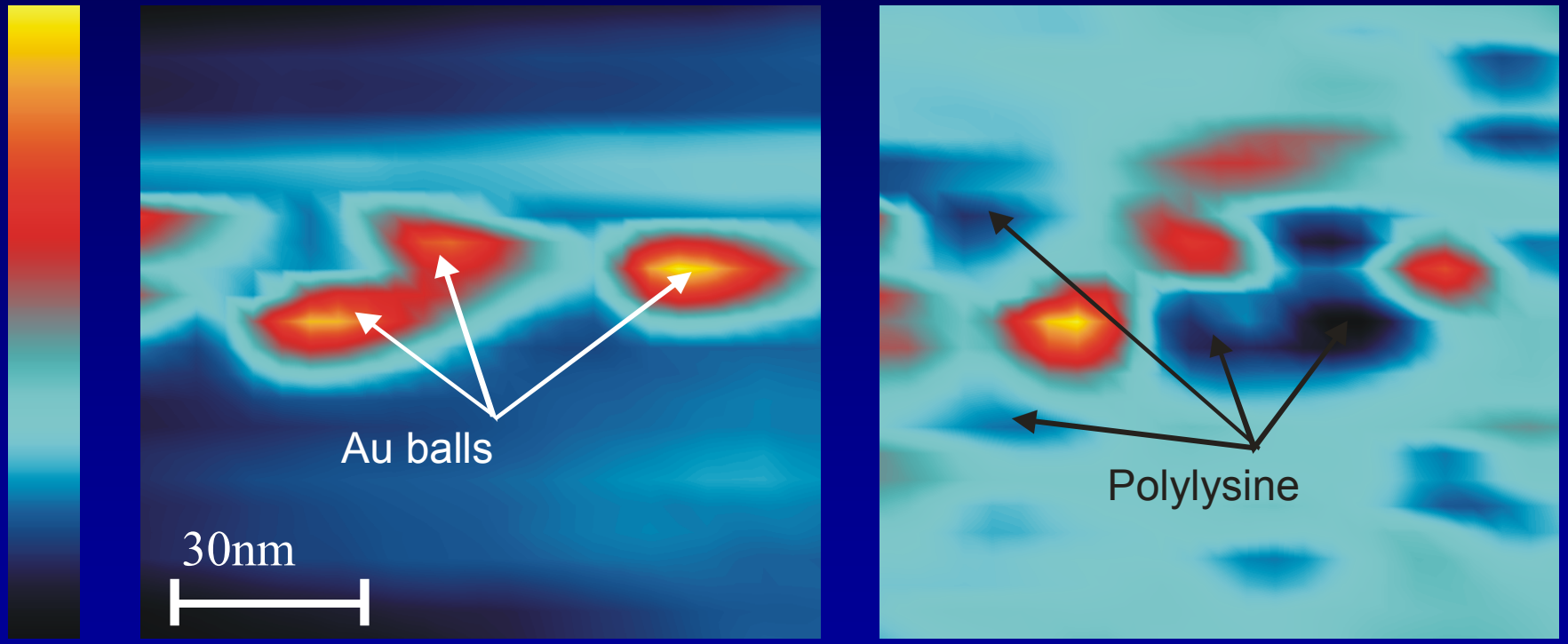

Resolution is limited only by the tip of the cantilever <u>not</u> by the wavelength

Lateral resolution correpsonds to λ/100 !!

Scanning nearfield infrared microscopy (SNIM)
Imaging of sub-surface structures

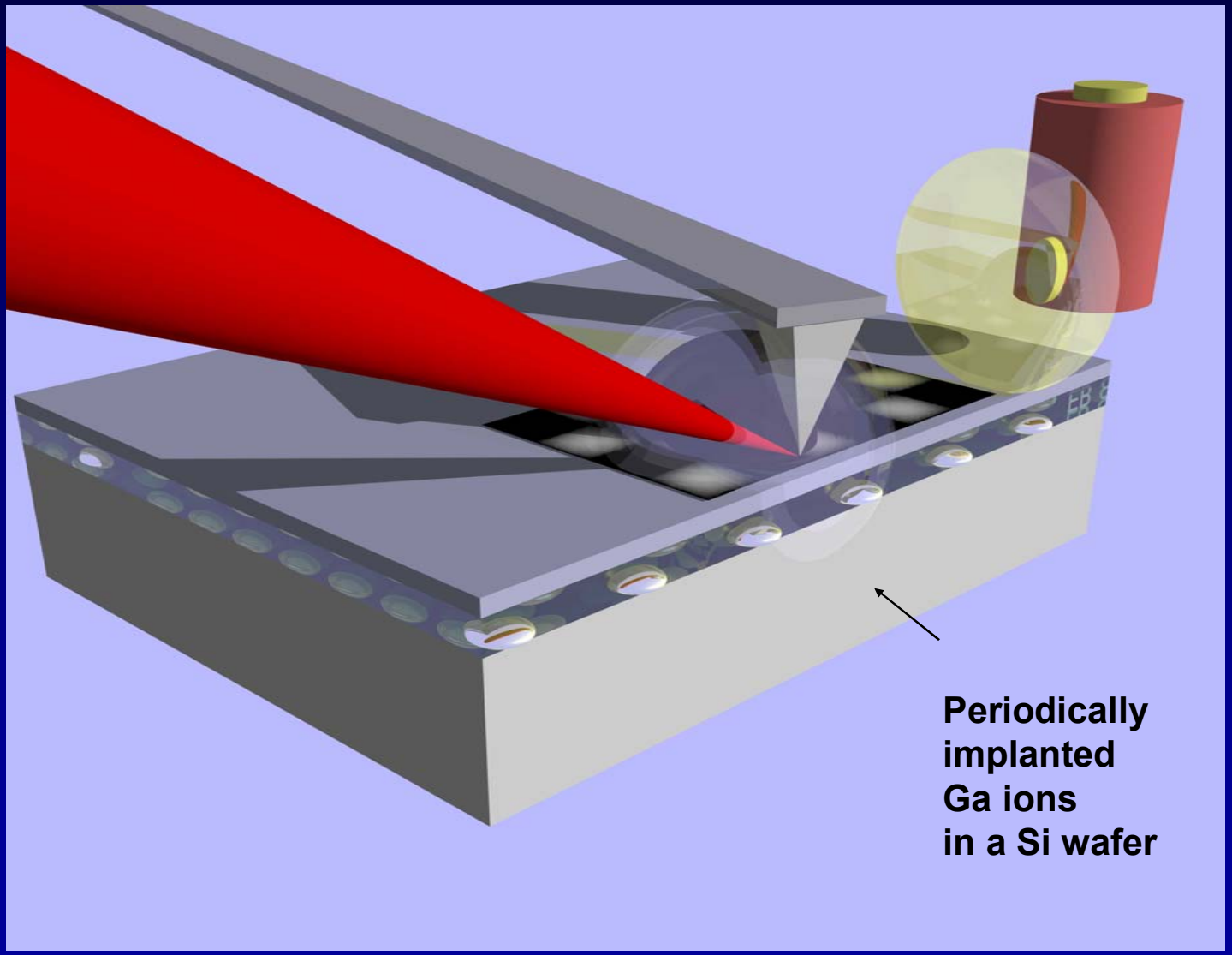

Imaging with a „chemical nanoscope“
Observation of subsurface structures

(*Phys. Chem. Chem. Phys.* **8**, 753 - 758 (2006))

AFM

SNIM

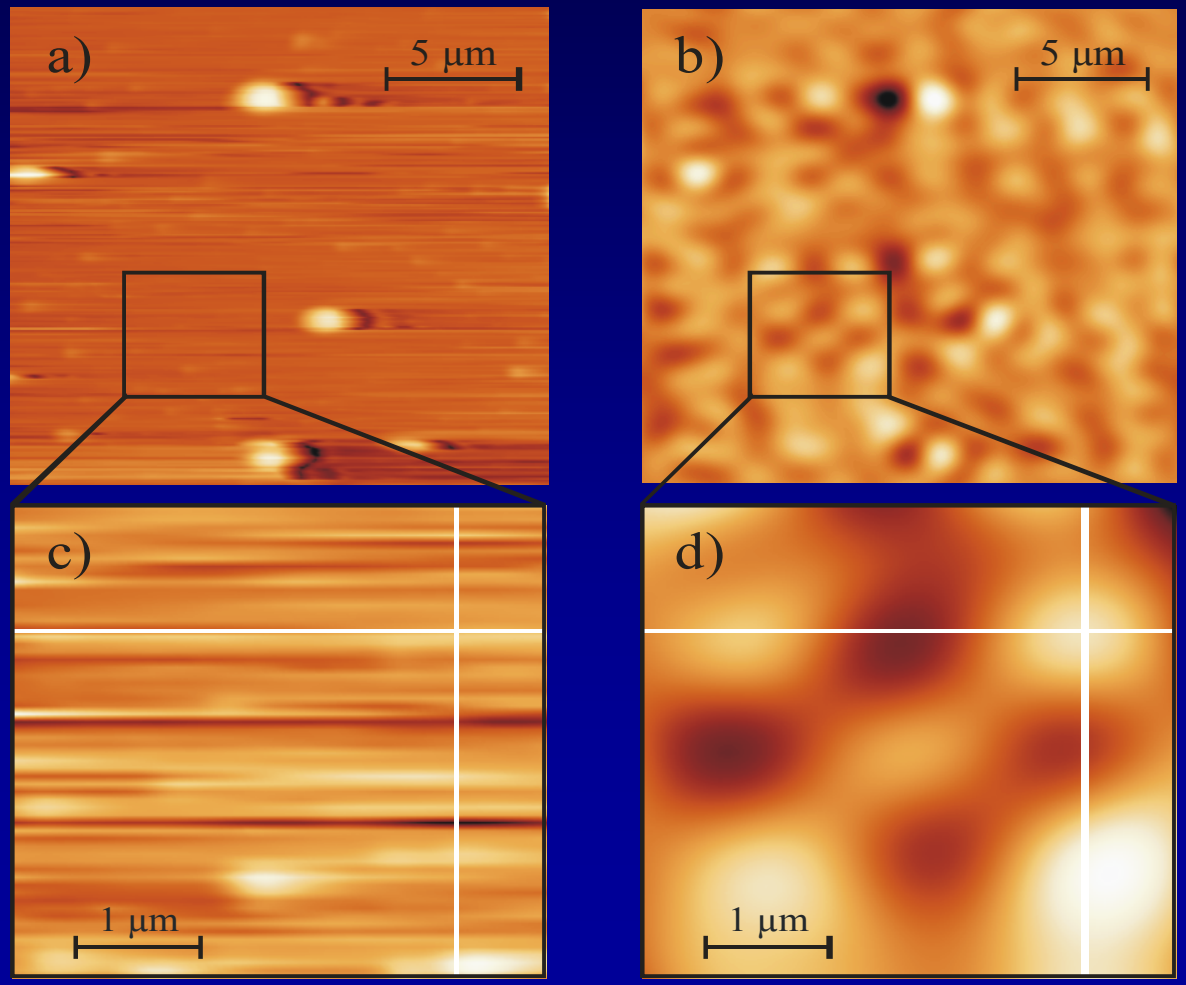

Measurement of implanted Ga-ions in a Si wafer

Ga:Si

$N(Ga)=4{,}4.10^{19}cm^3$

$\lambda=3{,}22\ \mu m$

Chemical imaging of monolayers

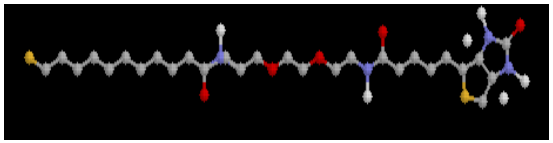

biotinylated alkylthiol (BAT)

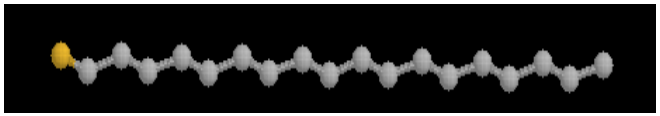

1-octadecanthiol (ODT)

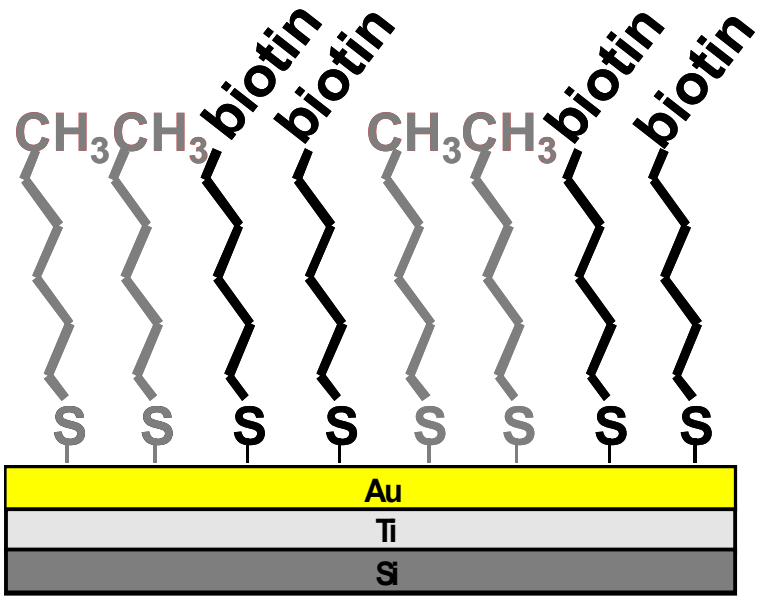

Electron microscope image of stamp and structured surface

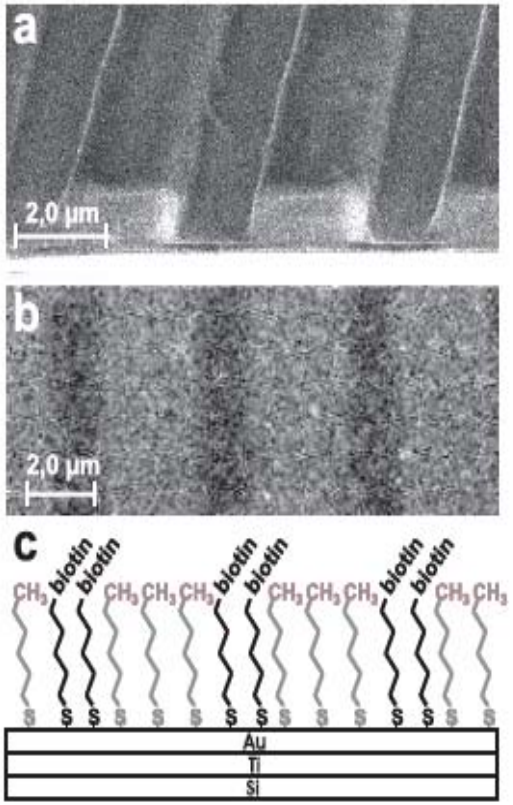

FIG. 3: Kopf et al.

PDMS stamp

IR spectra of distinct functional groups

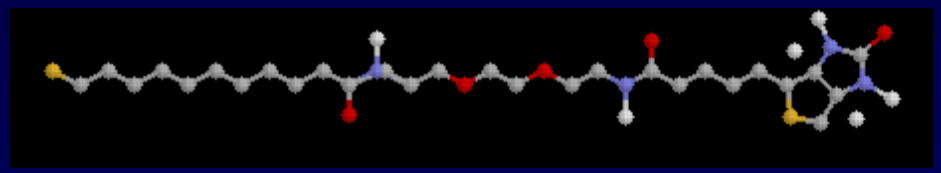

biotinylated alkylthiol (BAT)

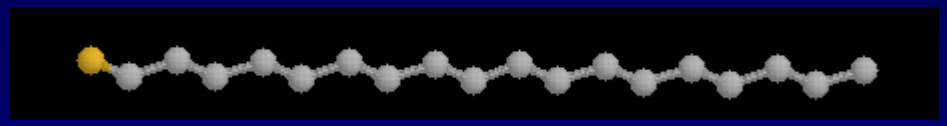

1-octadecanthiol (ODT)

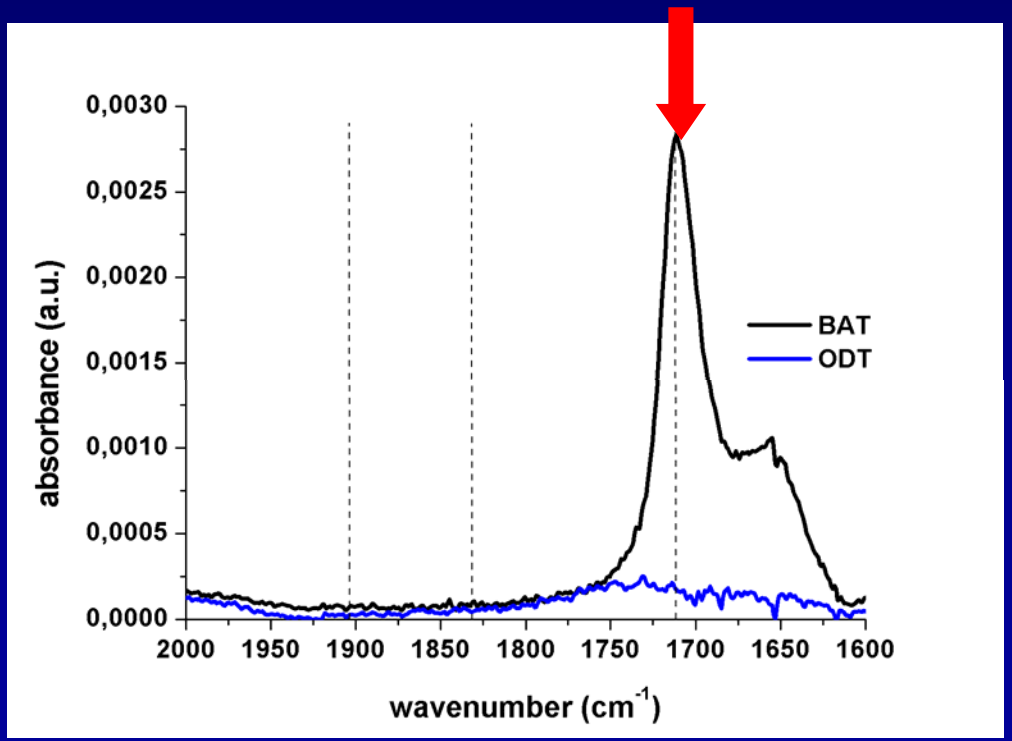

C=O band of ureido group at 1710 cm^{-1}

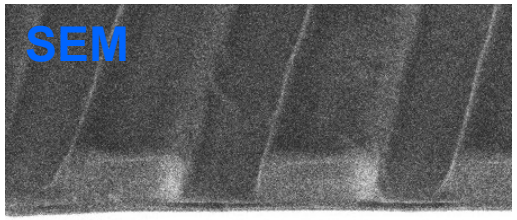

Experimental results

topography

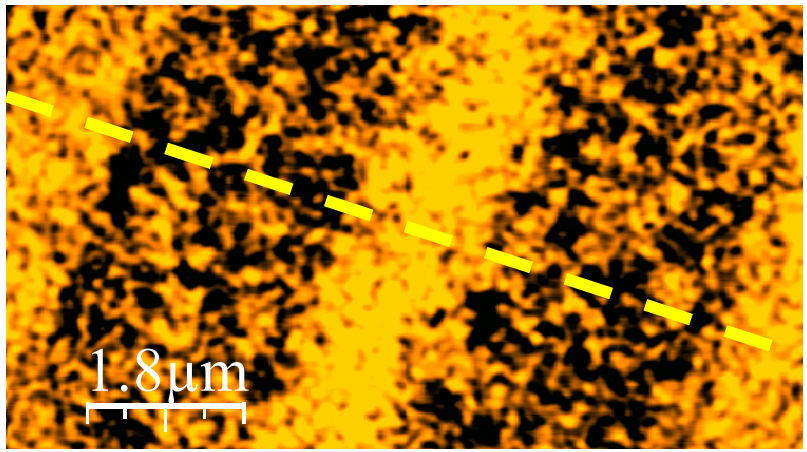

near-field

(1711 cm^{-1} – ureido absorption)

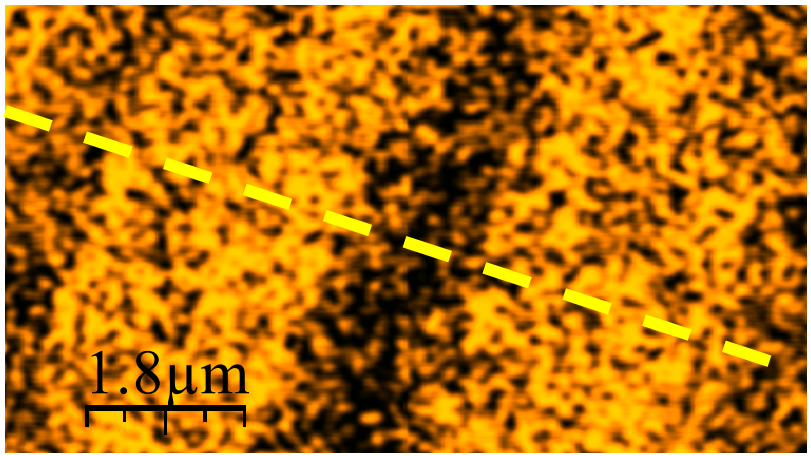

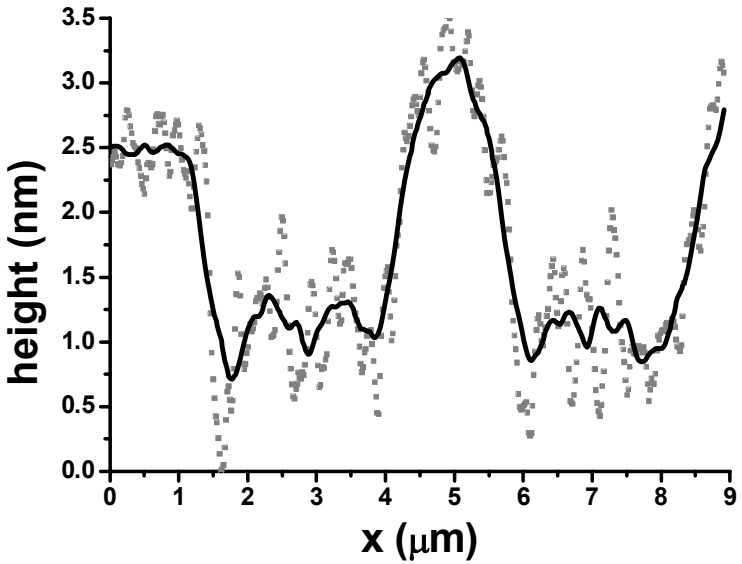

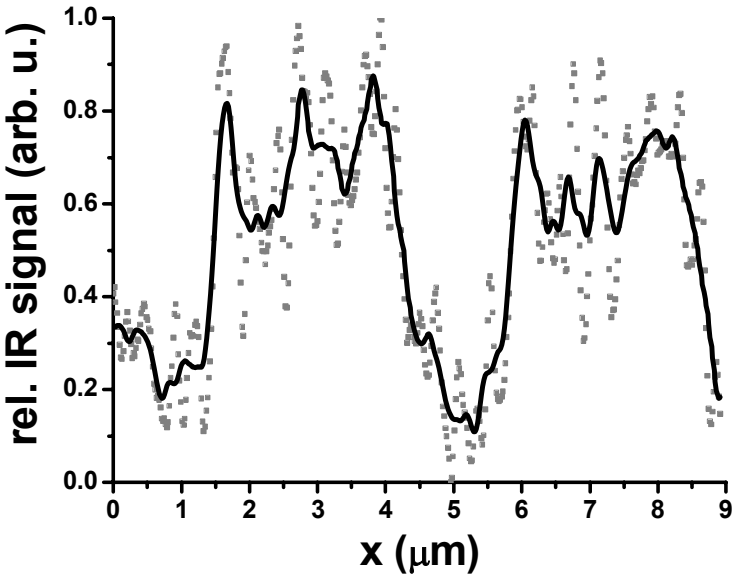

A „chemical nanoscope“
Fingerprint spectra with nm lateral resolution

(Kopf, Samson, Wollny, Grunwald,Bründermann and Havenith,

J. Phys. Chem. C 111, 8166-8171 (2007))

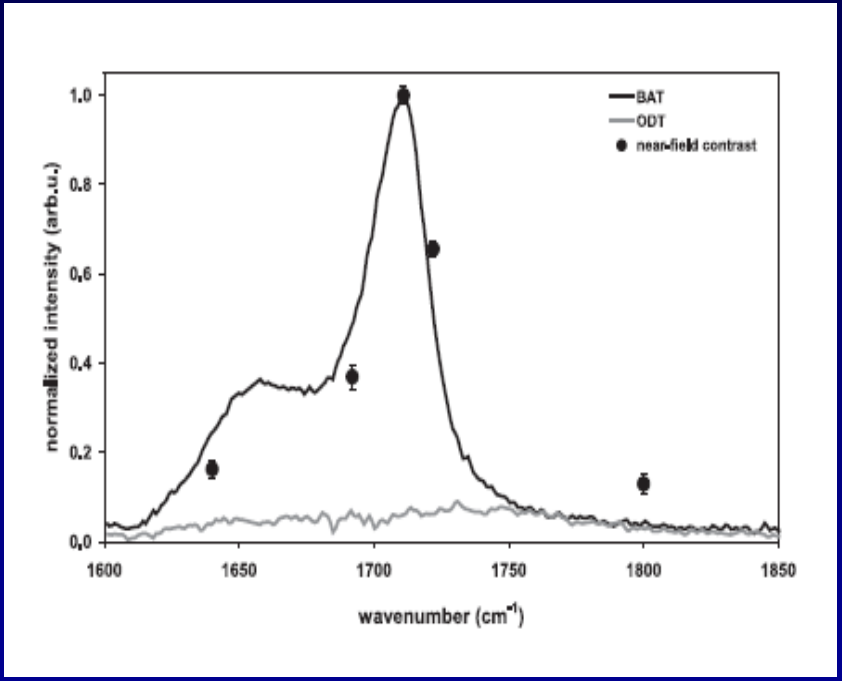

Detection limit: 5 10^{-20} mol/90 mm^2
27 attogramm

Contrast mechanism:
Dipole- mirror dipole coupling:
$\alpha^{mirror} = \beta\ \alpha^{tip}$; $B = (\varepsilon^{probe}-1) / (\varepsilon^{probe}+1)$

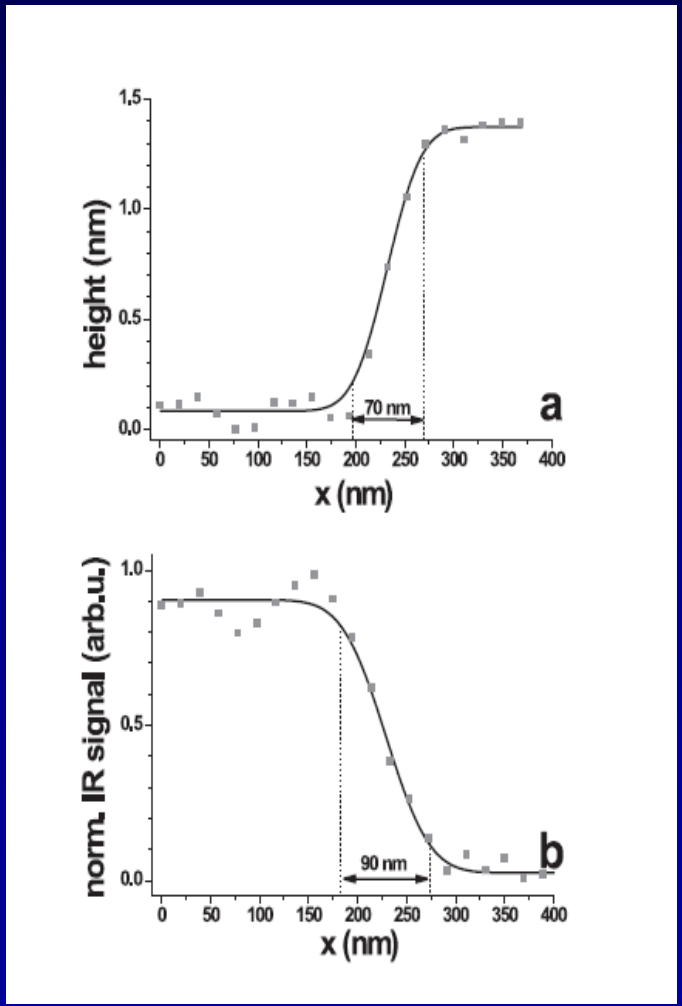

New project:
Taking a closer look (an infared image) at lipid rafts ?

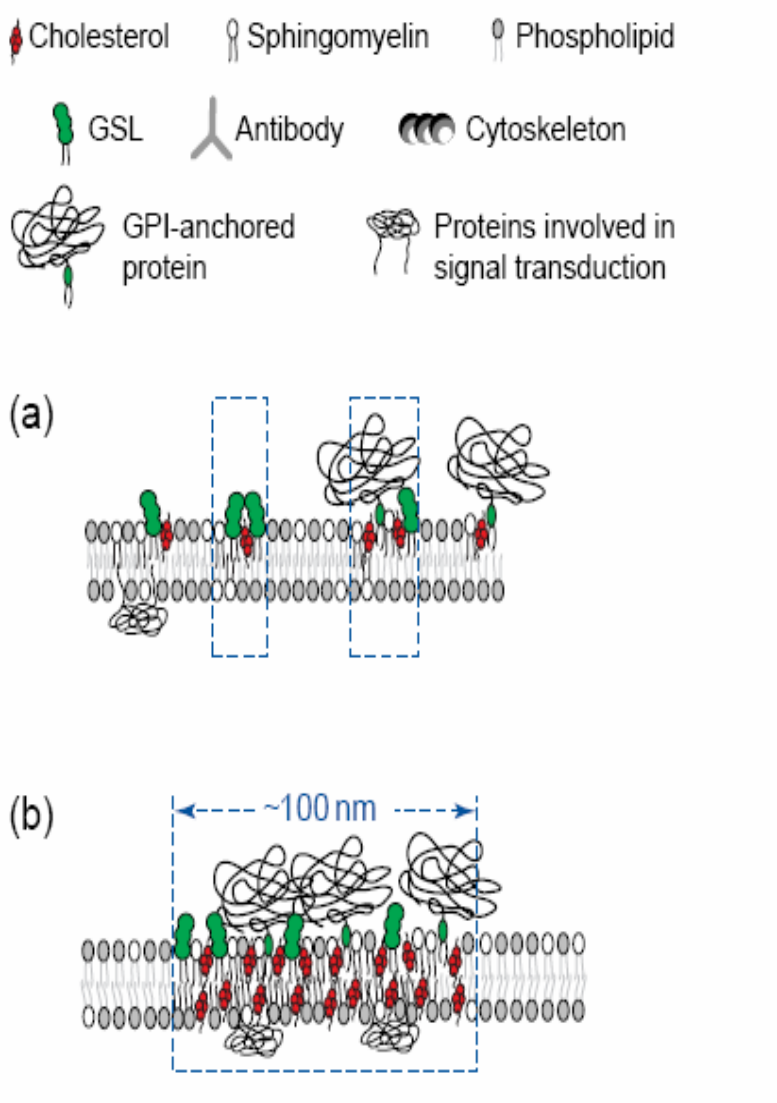

K. Jacobsen, C. Dietrich,
Trends in cell biology, 9, 88 (1999)

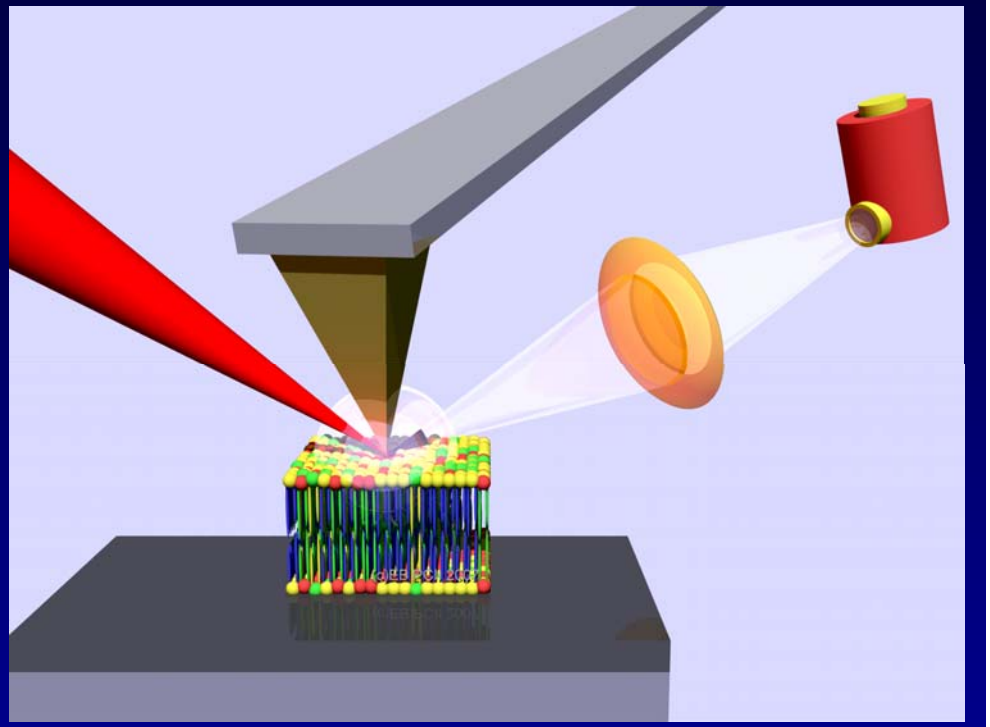

Possible lipid microdomains (rafts) in the plane of the plasma membrane. In these diagrams, lipids in the liquid-ordered phase have black, bold acyl tails; the normal bilayer is in liquid-disordered phase, where lipids are depicted as having grey acyl chains. Cholesterol distribution reflects only a relative enrichment in the liquid-ordered phase; molecules are not drawn to scale.

Artifical membranes

Dimeristylphosphatidylcholin (DMPC) und Cholesterin

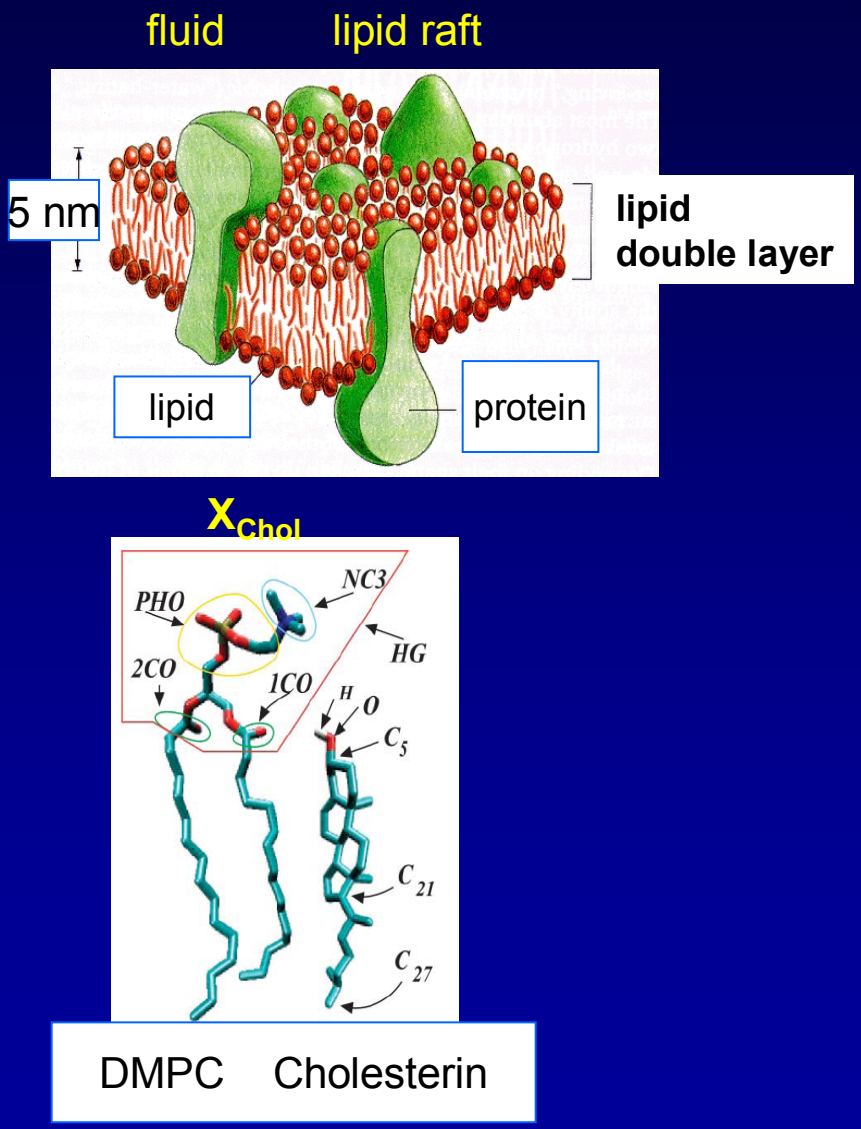

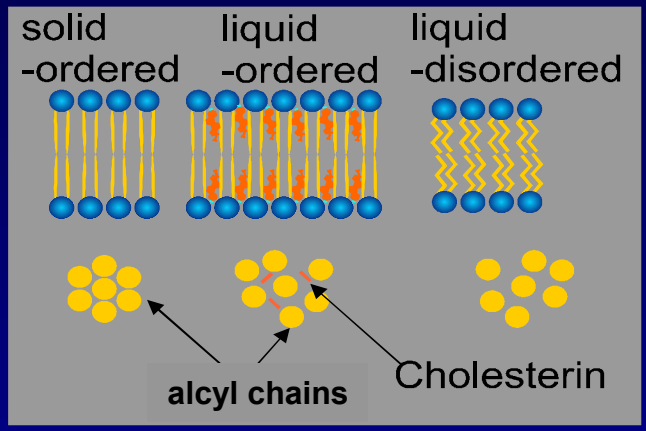

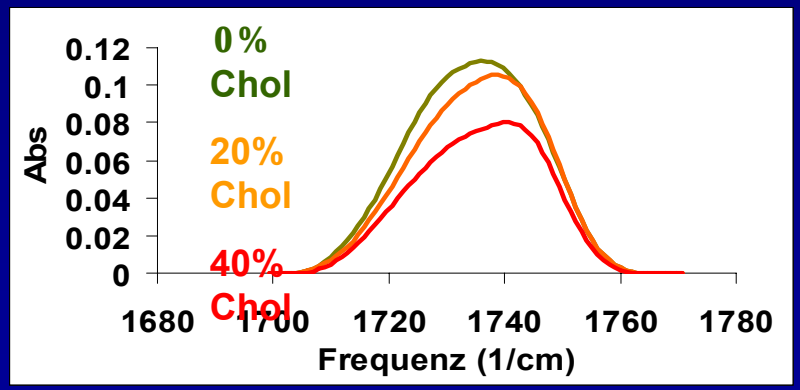

Z. Arsov et al. Chem. Phys. Lipids, 150:35–48, 2007.

Experimental set-up

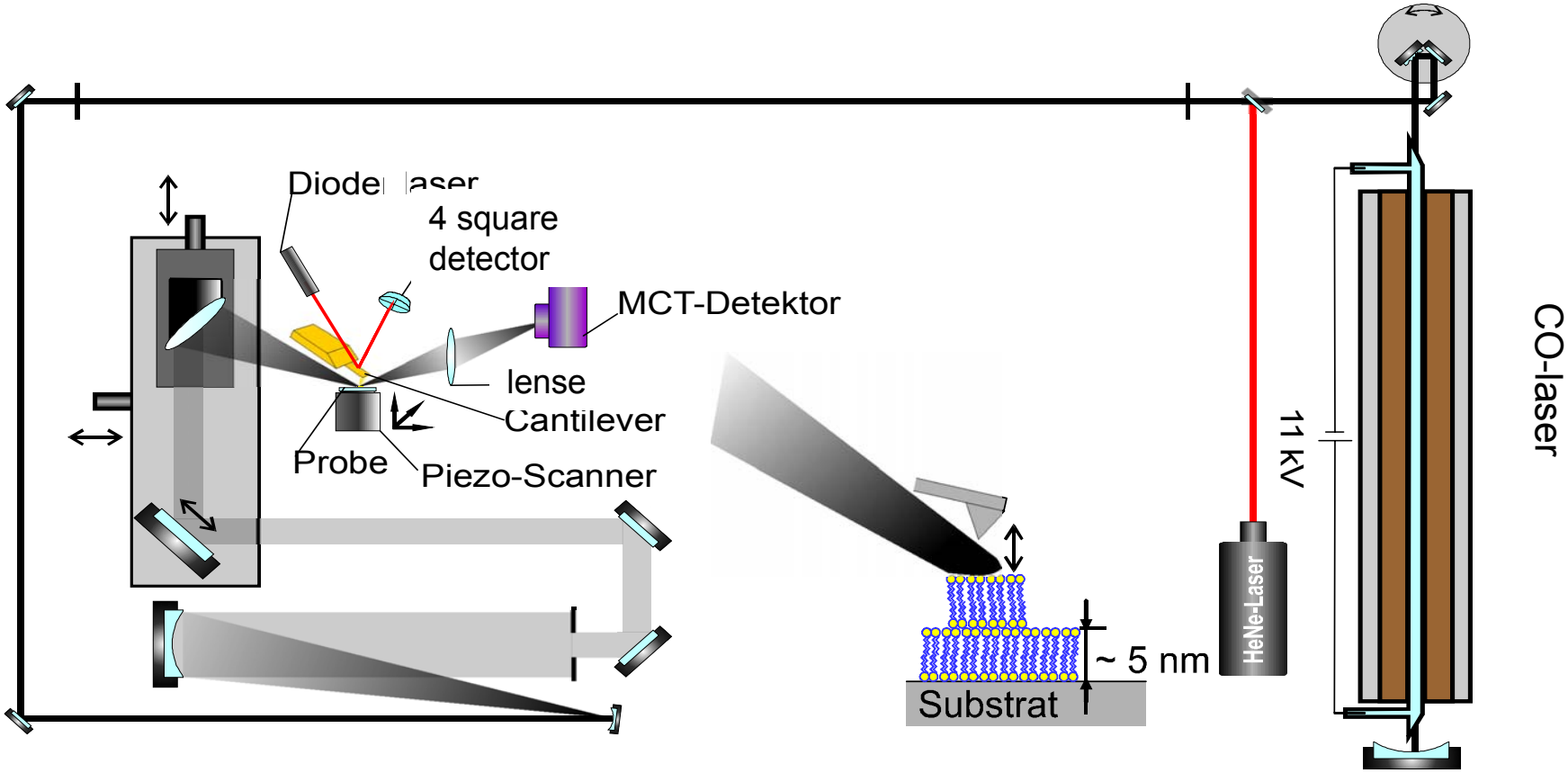

FTIR Spektren: DMPC

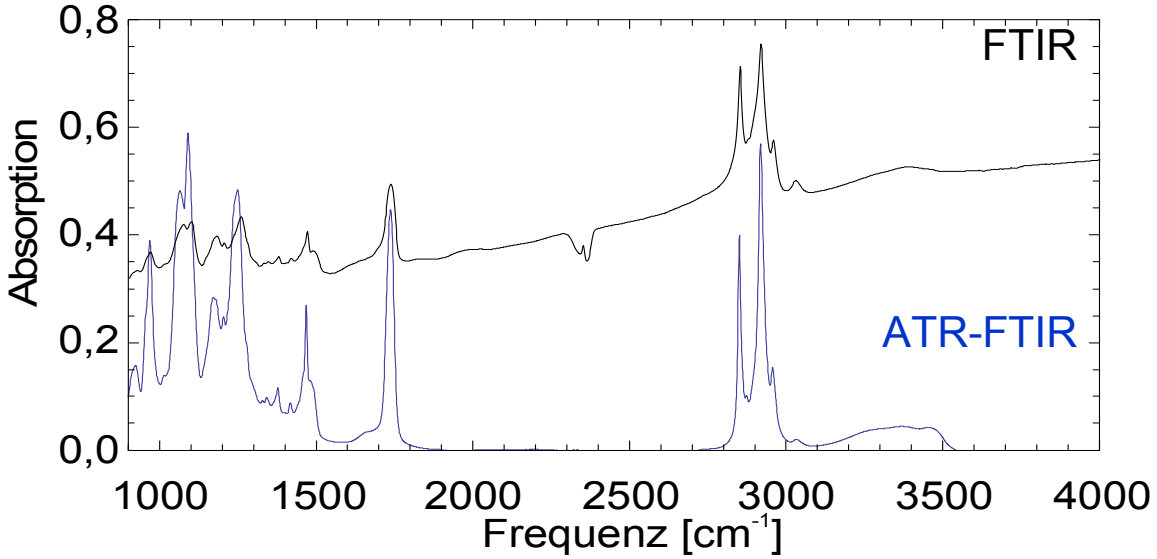

absorption refraction

$\longrightarrow \kappa \longrightarrow n \longrightarrow \varepsilon = n + i\kappa$

$\longrightarrow \alpha_{eff} \longrightarrow \sigma = k\,\mathrm{Im}(\alpha_{eff}) + \frac{k^4 |\alpha_{eff}|^2}{6\pi}$

abs. scattering

IR-near field microscopy of DMPC multilayer

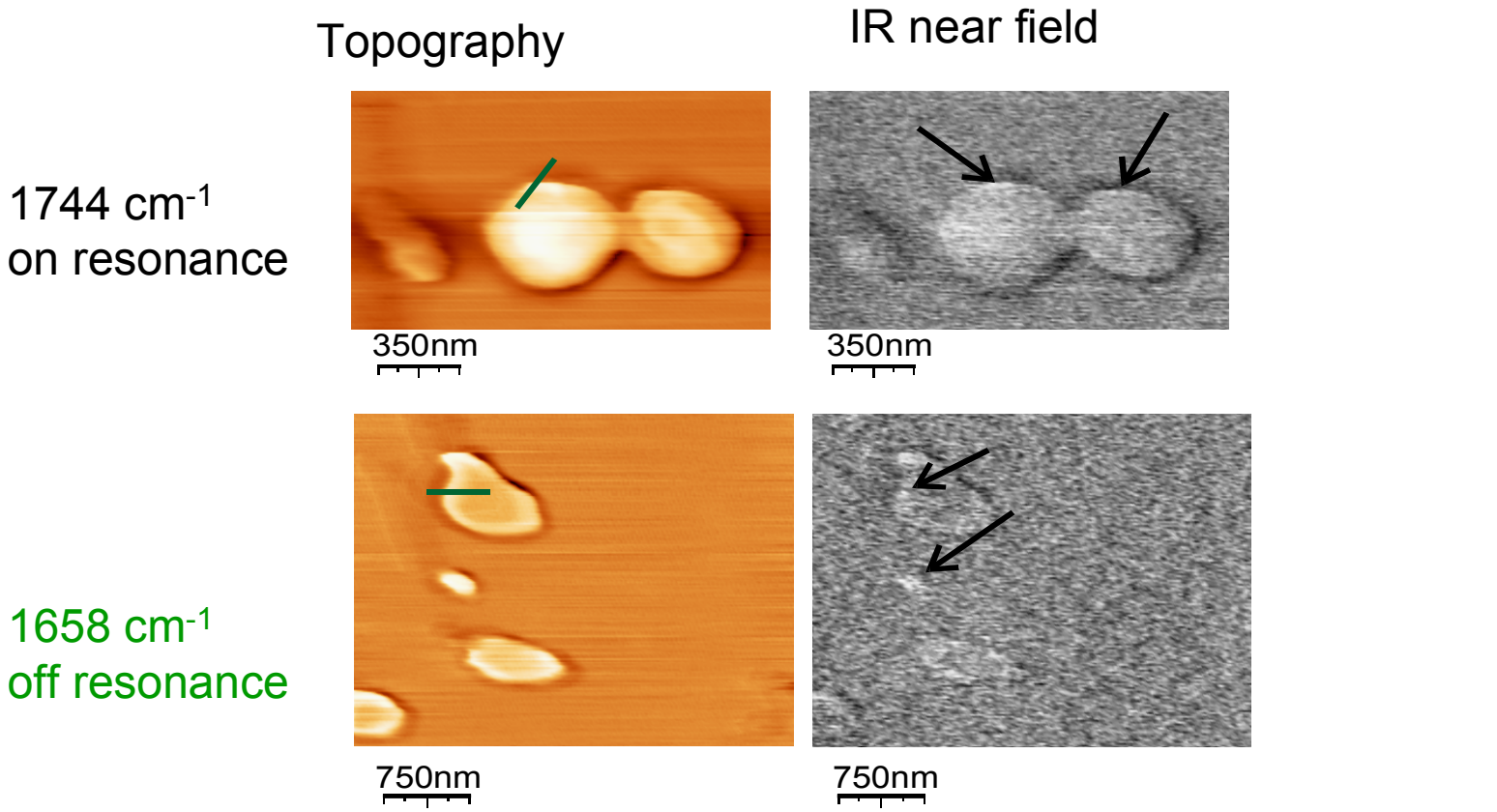

Lateral resolution 30 nm

DMPC multilayer and 30 nm gold ball on glimmer

IR near field: Lipid double layer

G. Wollny, E. Bründermann *et al.*

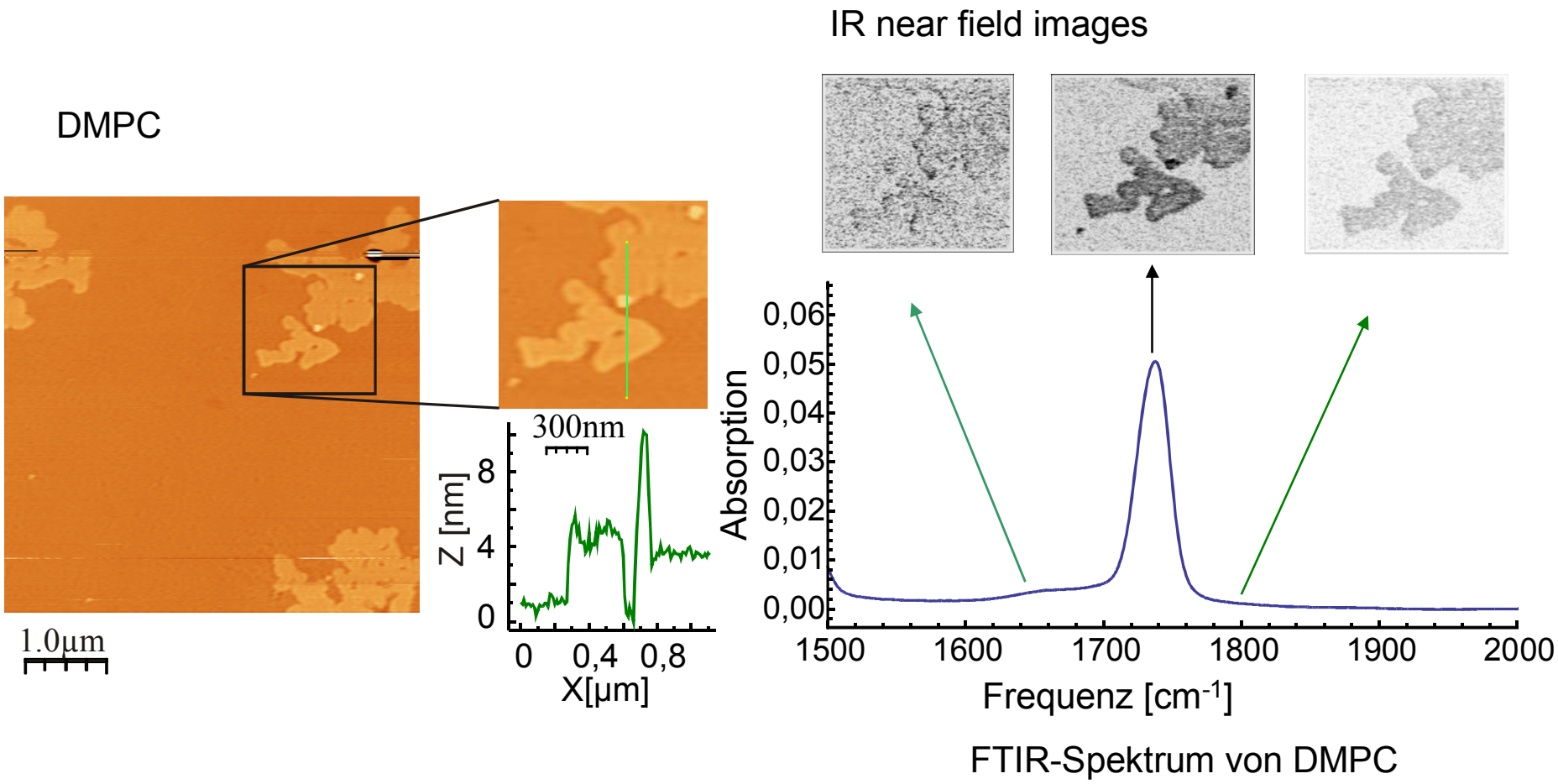

FTIR-Spektrum von DMPC

near field-contrast: DMPC on silicon

contrast

$$C = 1 - \frac{I_{DMPC}}{I_{Si}}$$

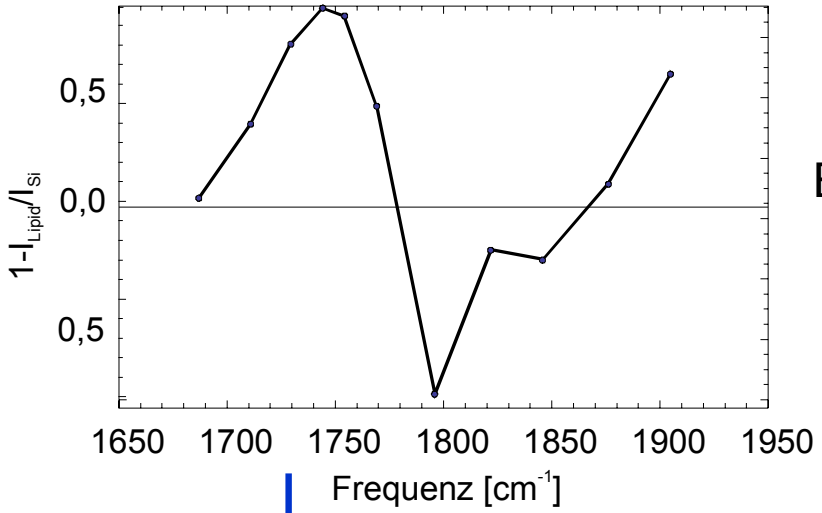

Experimental result

$$\sigma = k\,\mathrm{Im}(\alpha_{eff}) + \frac{k^4 \left|\alpha_{eff}\right|^2}{6\pi}$$

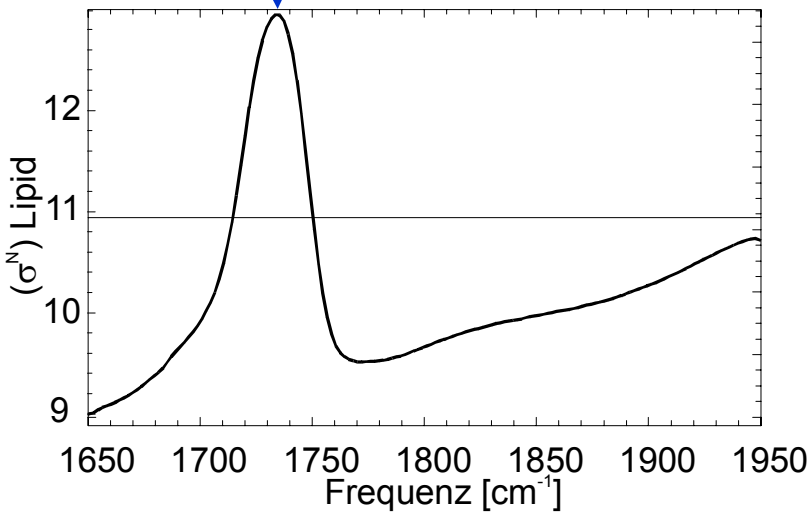

predicted
scattering cross section

IR near field spectrum of DMP double layer

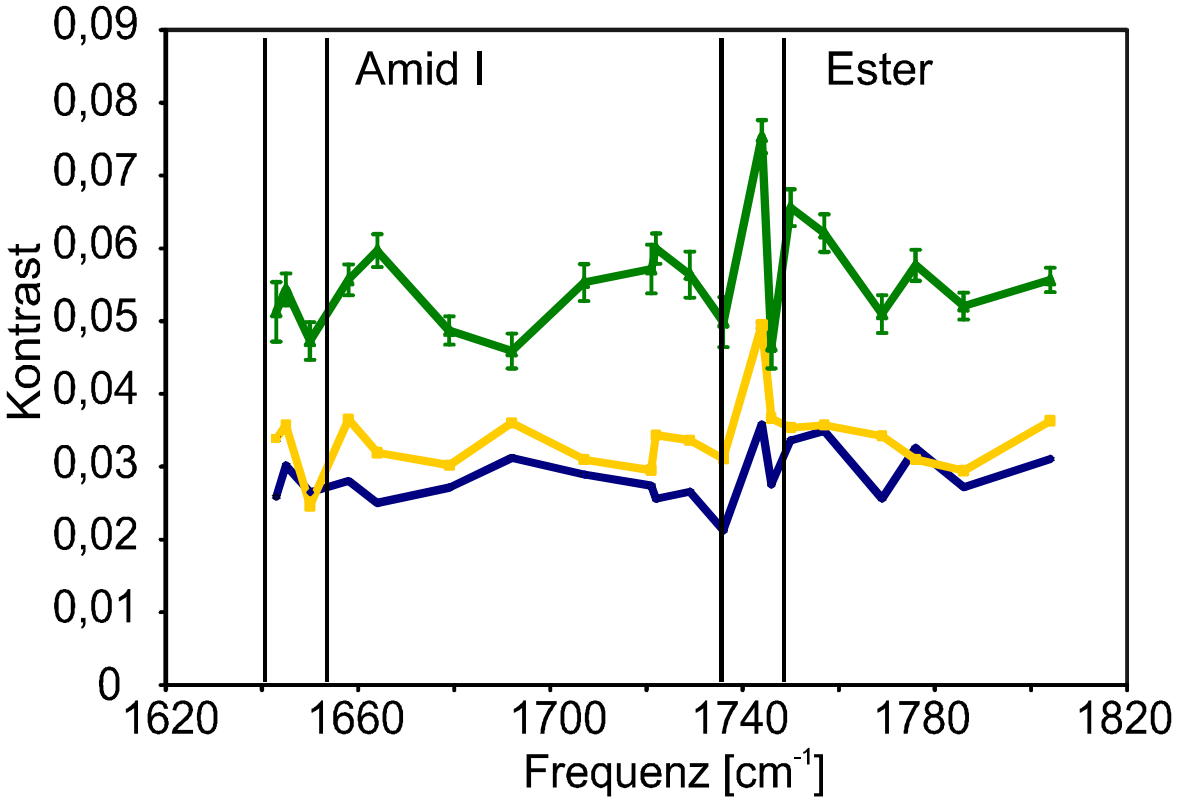

Chemical mapping of a surface

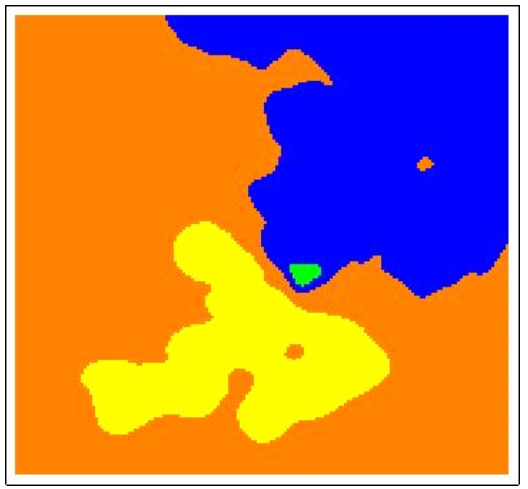

green: two lipid double layer (DMPC)
area: (90 nm)²

Corresponds to 320000 molecules

Taking a closer look (an infared image) of proteins in membranes

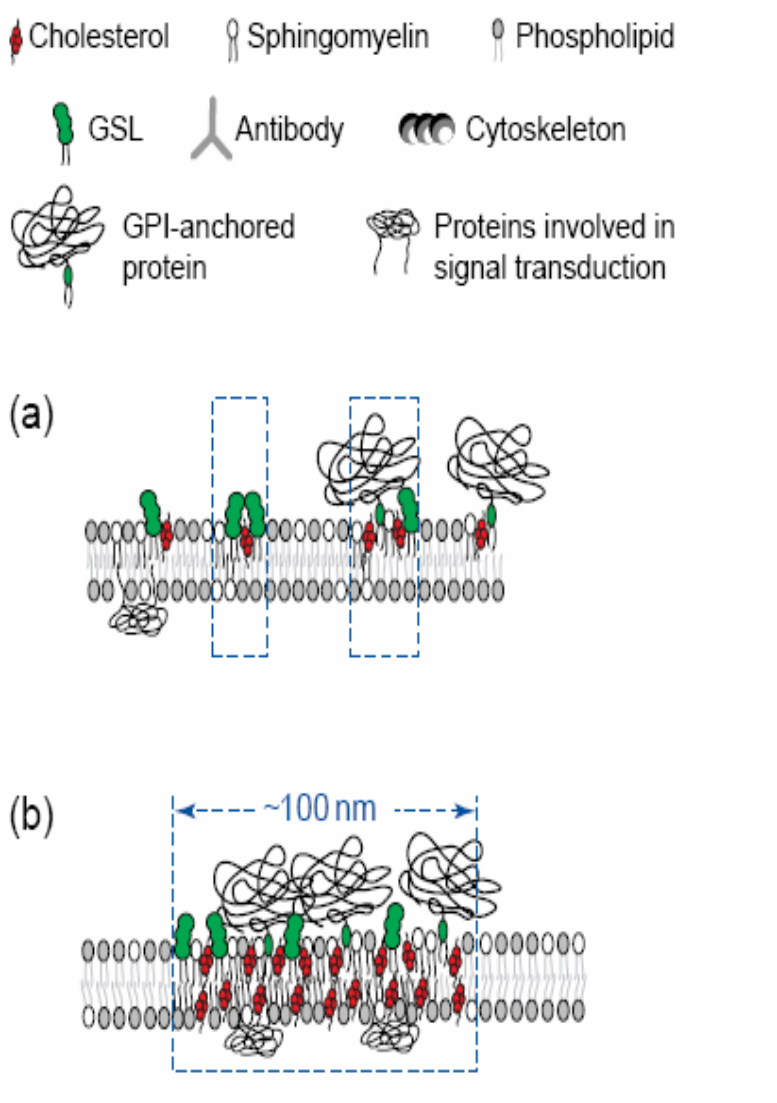

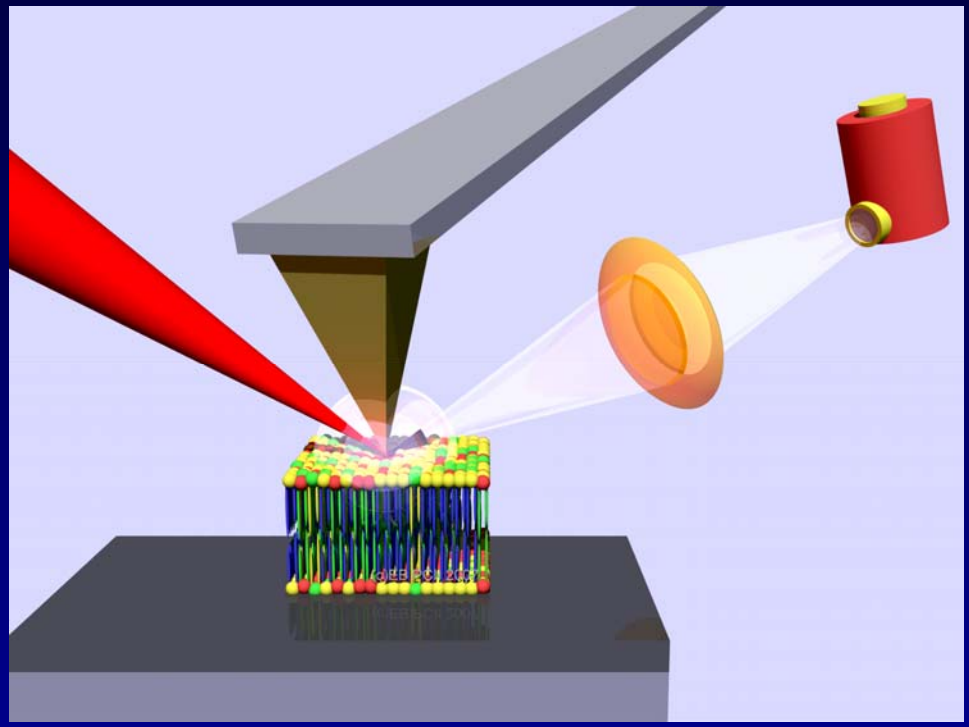

Possible lipid microdomains (rafts) in the plane of the plasma membrane. In these diagrams, lipids in the liquid-ordered phase have black, bold acyl tails; the normal bilayer is in liquid-disordered phase, where lipids are depicted as having grey acyl chains. Cholesterol distribution reflects only a relative enrichment in the liquid-ordered phase; molecules are not drawn to scale.

K. Jacobsen, C. Dietrich,
Trends in cell biology, 9, 88 (1999)

Imaging proteins in artificial membranes

Cooperation with Heberle group

512 ⊛ 512 dots

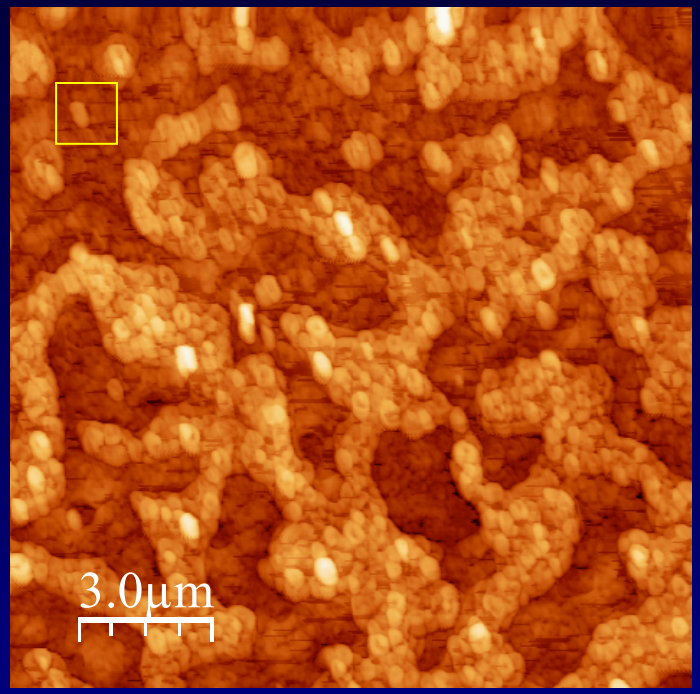

15 ❍m

15 ❍m

Each dot corresponds to ca. 30 nm

Topograpy
31⊛31 dots

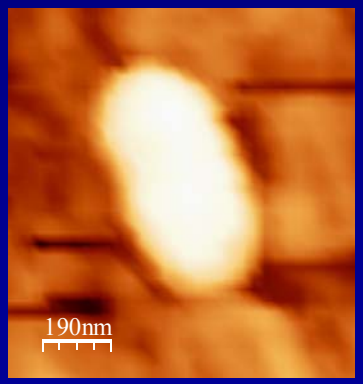

The bright spot has an extension of ca. 300-400 nm and a height of ca. 50 nm

1658 cm^{-1}

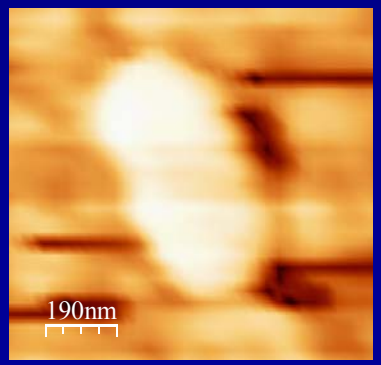

1740 cm^{-1}

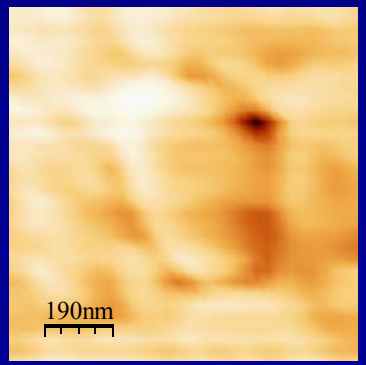

1804 cm^{-1}

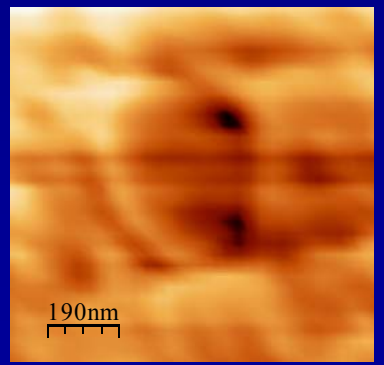

Near field-signals recorded with a tapping-mode-frequency of 172,8 kHz

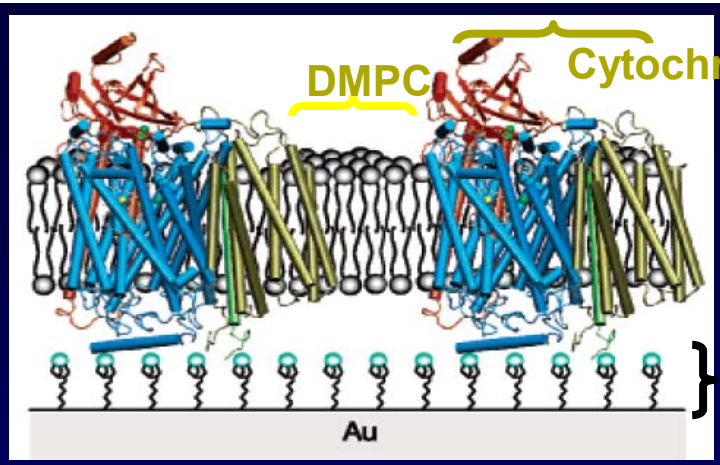

First experimental results

F. Ballout, I. Kopf, *et al*

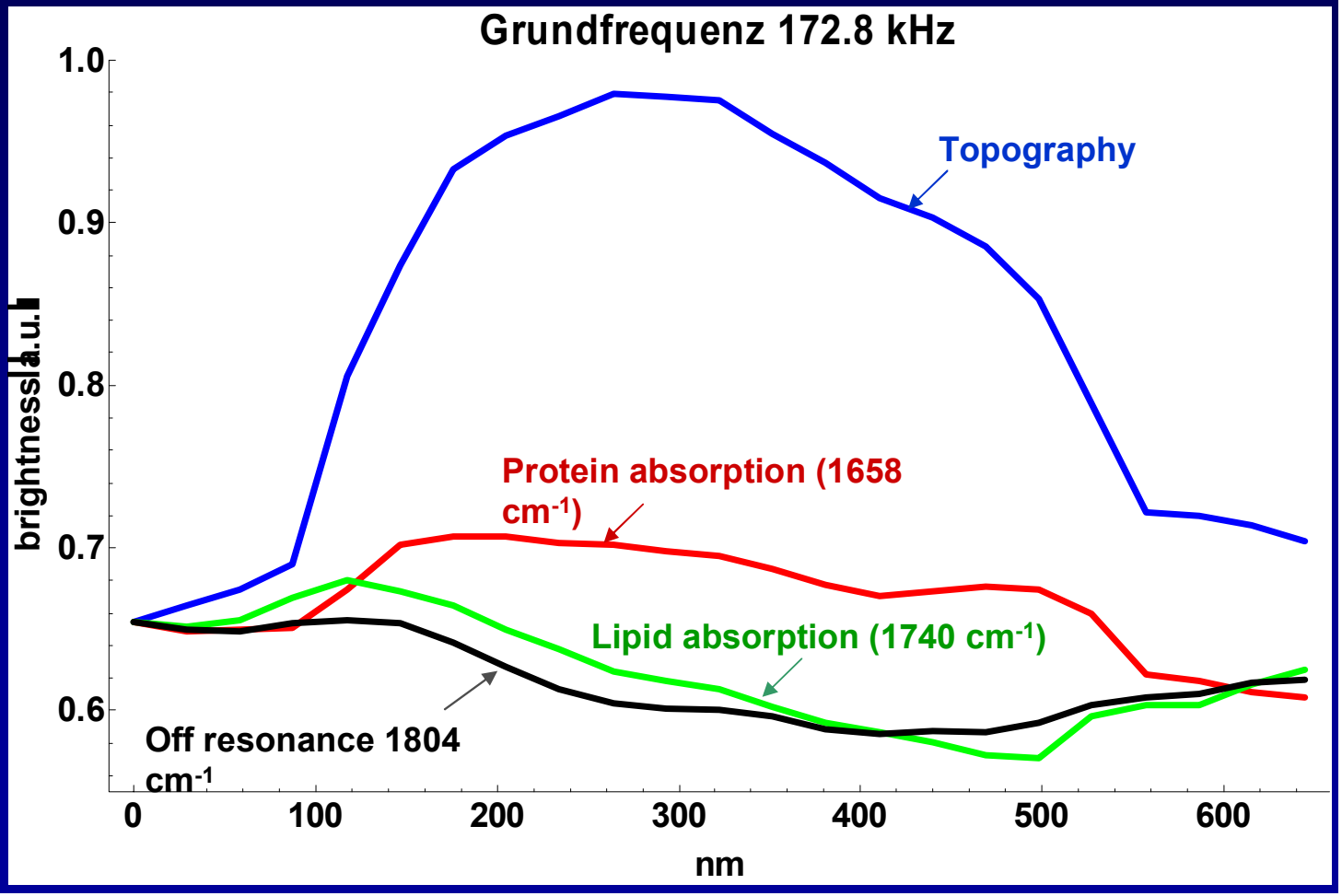

IR mapping of a single tobacco virus
Brehm, Taubner, Hillebrand, Keilmann
Nanoletter 6, 1308 (2006)

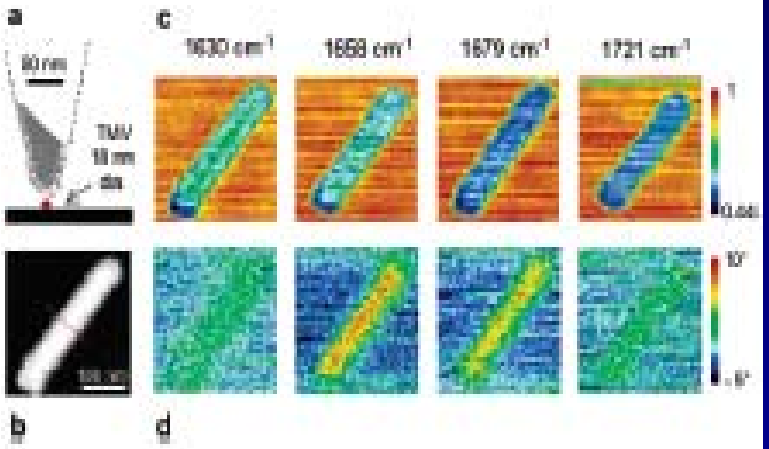

Figure 1. Infrared near-field images of a single tobacco mosaic virus (TMV) on Si. (a) Scale sketch of TMV under the probing tip, with inserted TEM micrograph of the actually used Pt-coated Si tip. (b) Topography. (c, d) Near-field amplitude and phase contrast images repeatedly recorded at different infrared frequencies as indicated.

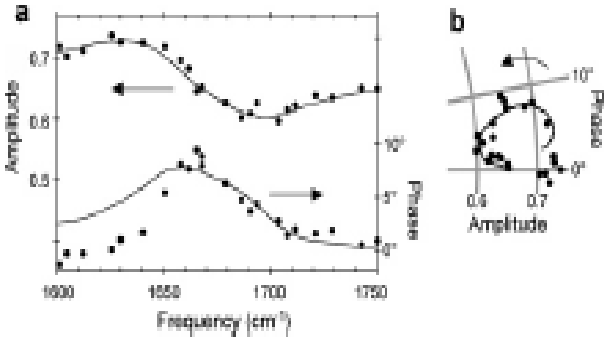

Figure 2. Infrared near-field spectrum of single TMV. The data points are extracted one each from many images such as in Figure 1c,d, as averages over the TMV's interior. (a) Amplitude and phase contrast relative to Si. (b) A polar display of amplitude vs phase contrast testifies to the resonance character of the near-field spectrum. The curves represent a model prediction.

Imaging of DNA nano arrays cooperation with ELETTRA, Trieste

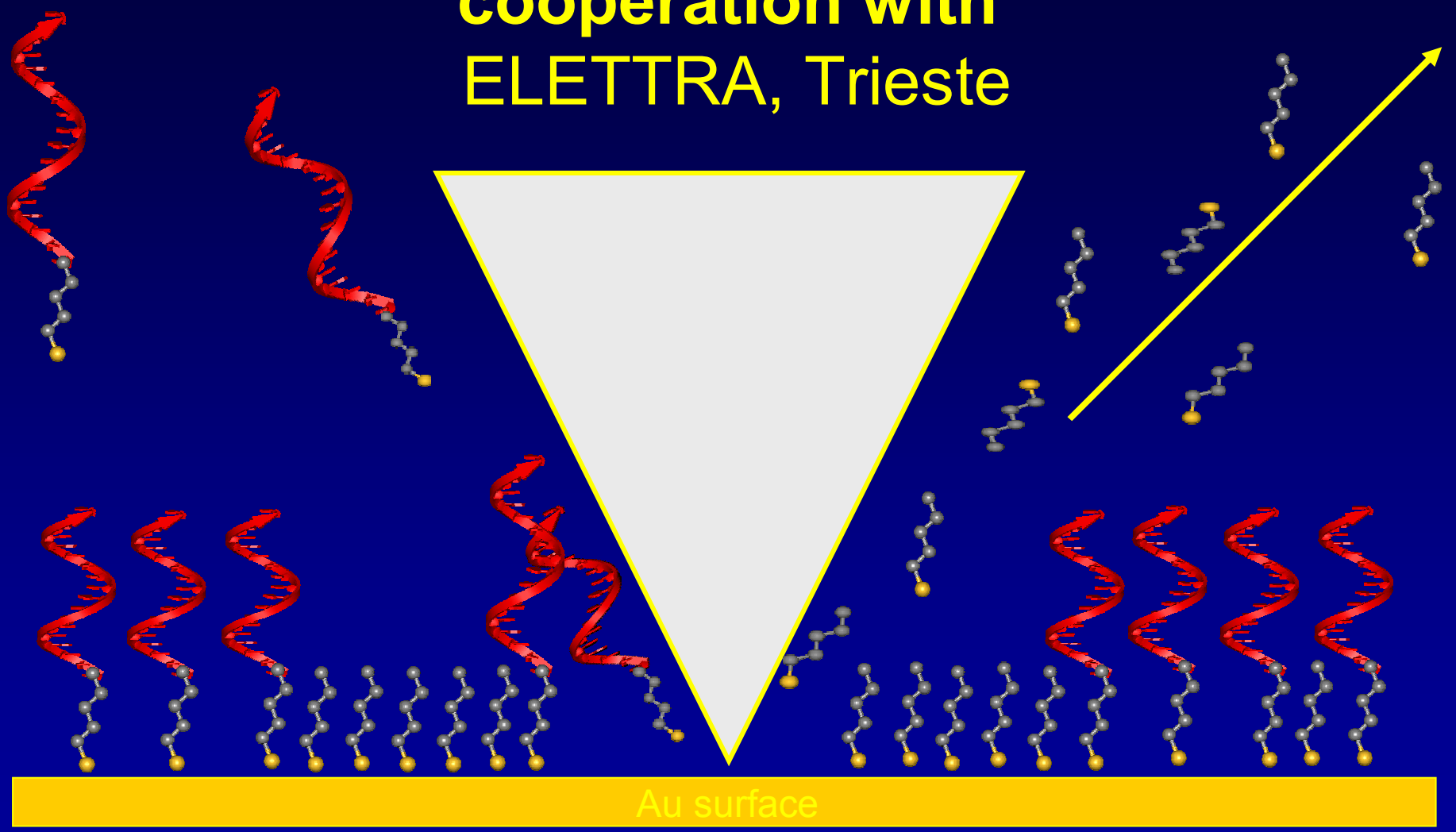

Distinction between single and double stranded DNA on a nano scale

IR-nearfield Measurements of single and double stranded DNA

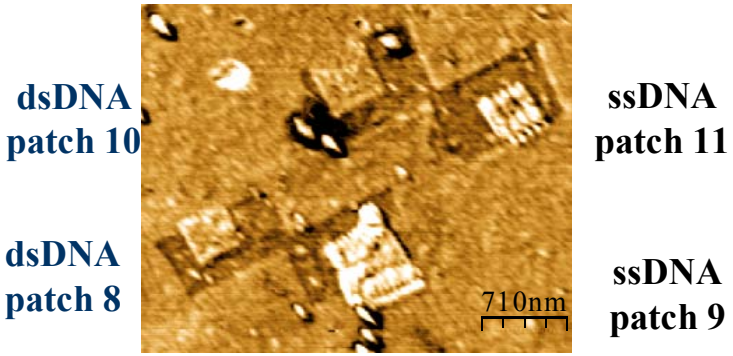

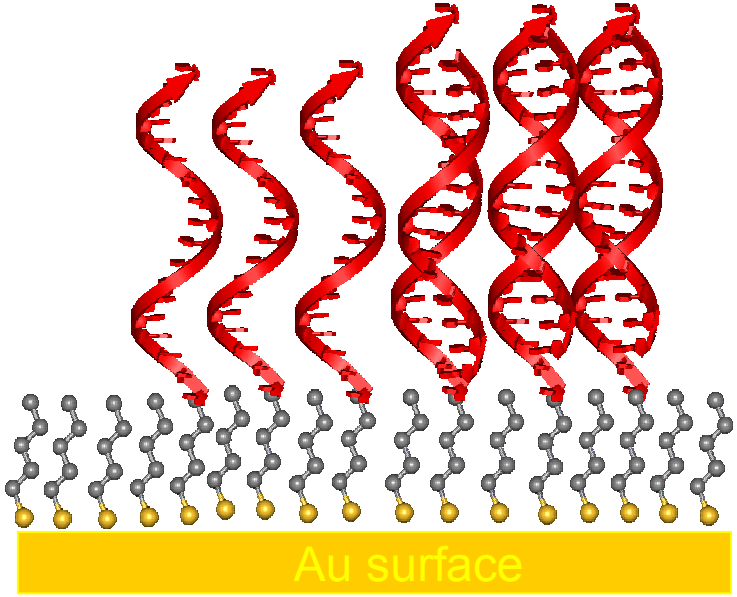

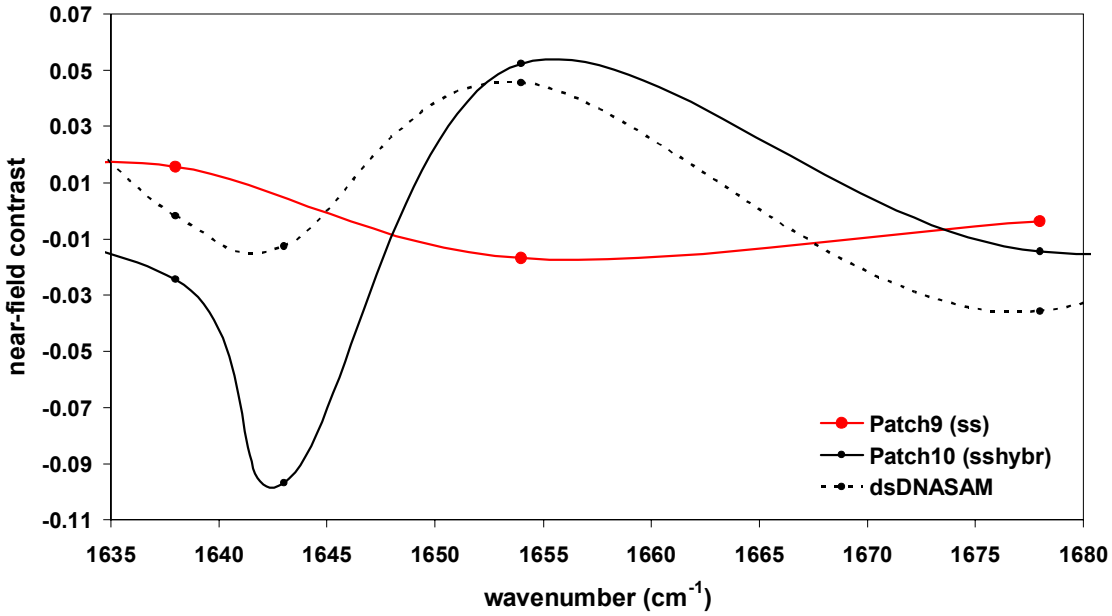

I. Kopf *et al*

Chemical mapping of nano particles
Cooperation with plasma physics (J. Winter, RUB)

Core:

- Diamond-like stucture (DL)
- Hard material
- No water
- 50-100 nm diameter

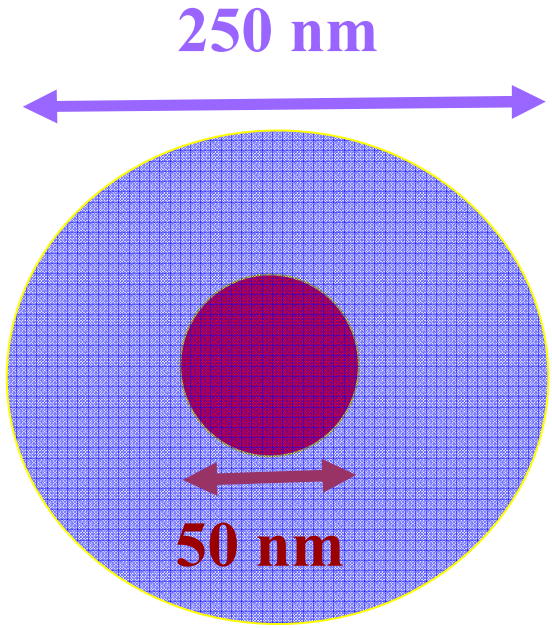

Shell:

- Polymer-like structure (PL)
- Soft material
- Intersticial water
- Diameter depends on growing time (450 nm)

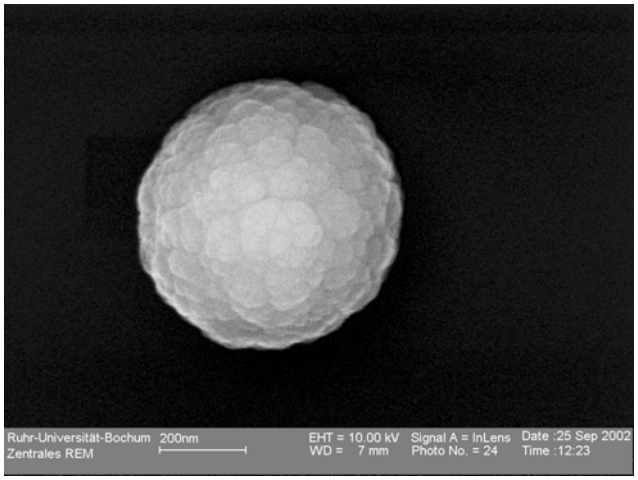

PL nanoparticles (450 nm)

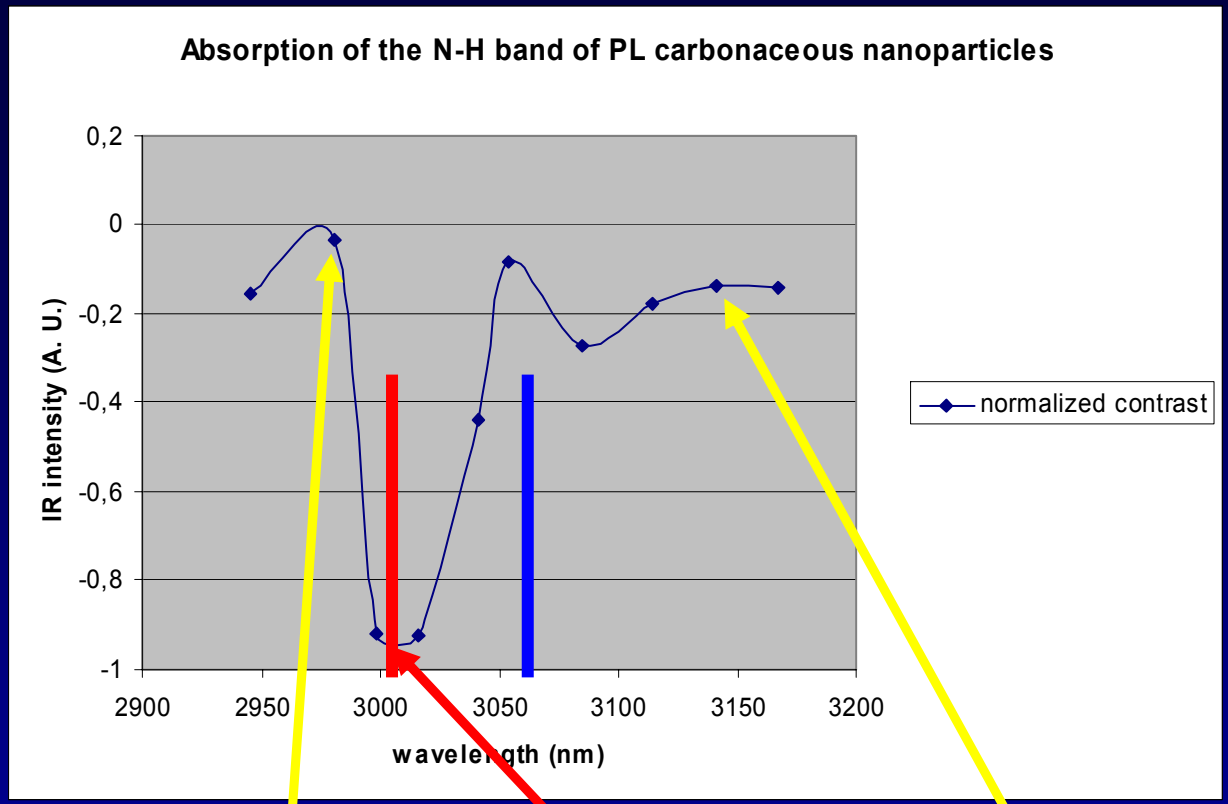

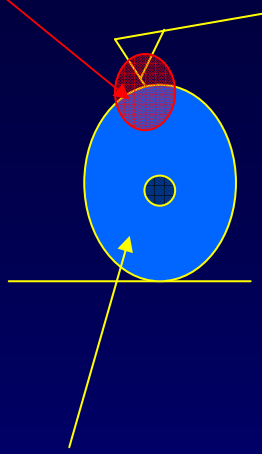

J. Sebastian *et al*

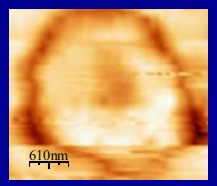

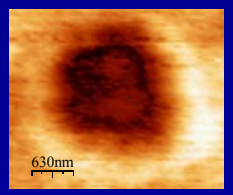

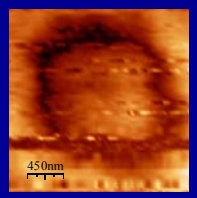

2981 nm 3016 nm 3141 nm

DL nanoparticles (56 nm)

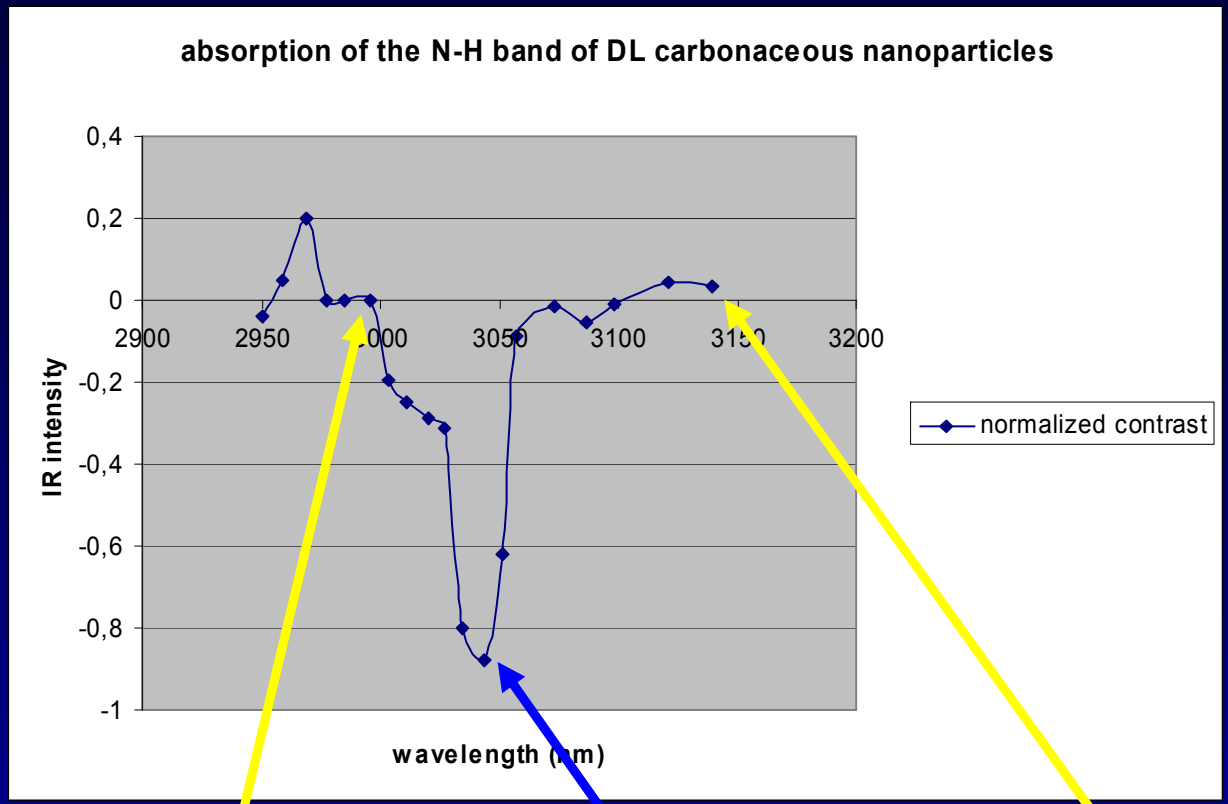

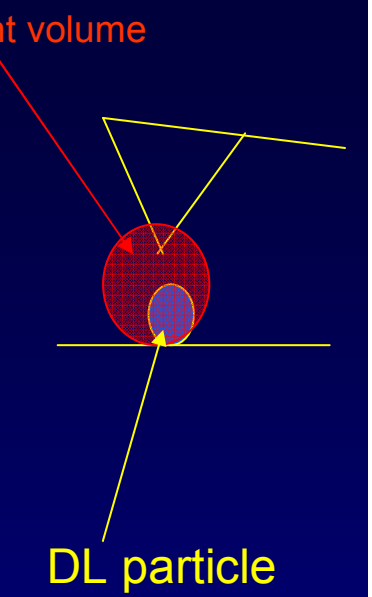

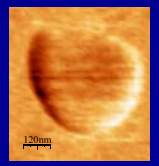

2998 nm

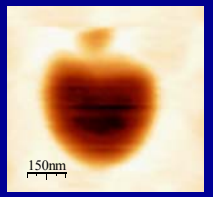

3051 nm

3148 nm

In comparison:
IR spectra of diamond like and polymer like nano particels

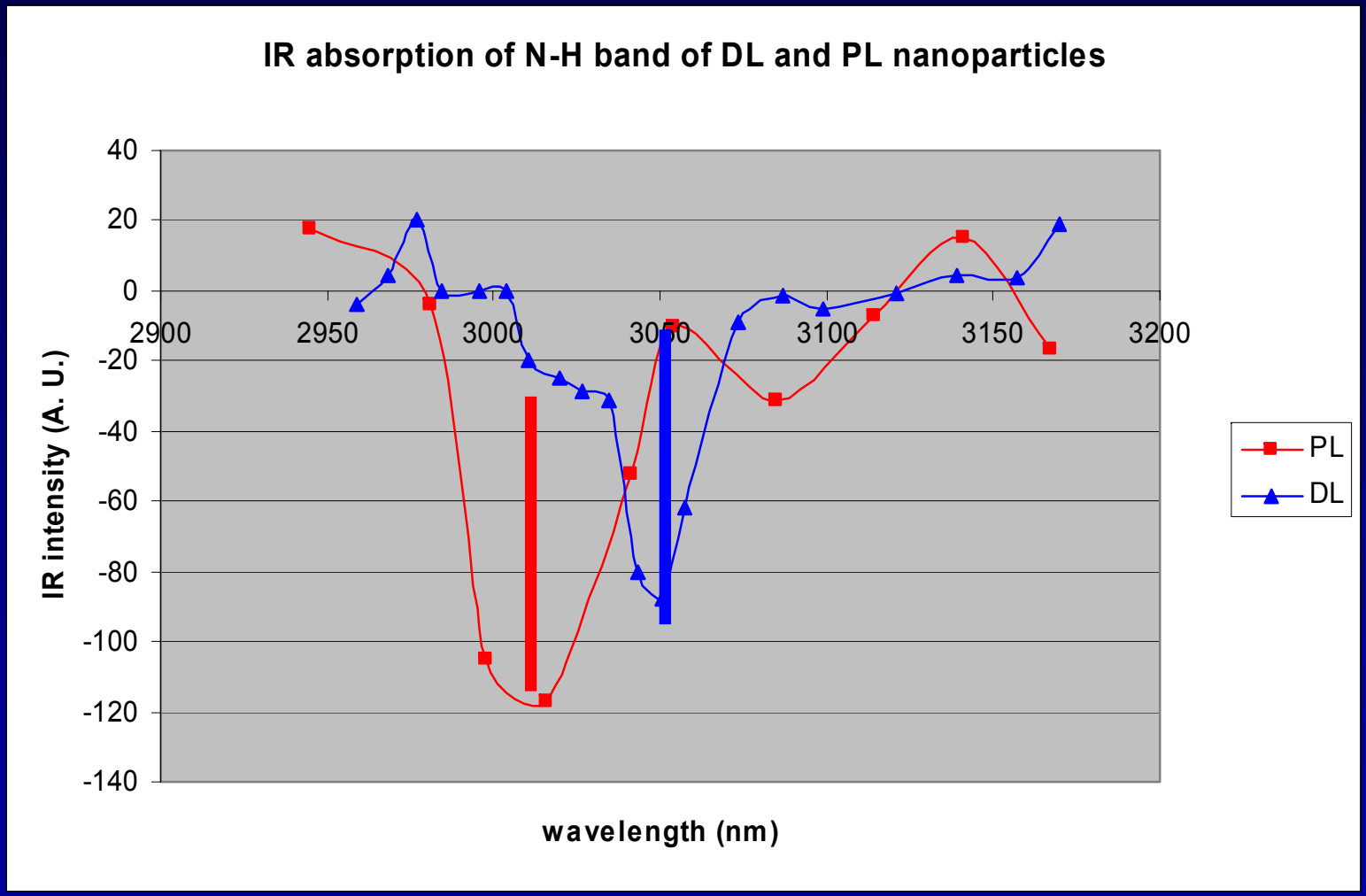

J. Sebastian *et al.* cooperation with J. Winter , RUB

Summary
Chemical Imaging on the nm scale

- Set-up of a „chemical nanoscope“ (SNIM) using new IR laser sources in the amid, C-H and O-H spectral region
- Chemical Imaging without the need of extrinsic labels
- Demonstration of high lateral resolution (10 nm)
- Sub-surface structures can be imaged (up to 100nm)
  penetration depth scales with wavelength
- IR spectra of 30 nm x 30 nm area can be recorded
- High detection sensitivity:
  Observation of monolayers
- Detection limit:
  4 molecules/nm^2 ($6.6 \cdot 10^{-24}$ mol/nm^2)
- Observation of protein in membranes or lipid rafts ?

Aufbau einer leistungstarken Strahlungsquelle im IR Bereich

High power IR-radiation
IR-cw OPO (2.9 W)

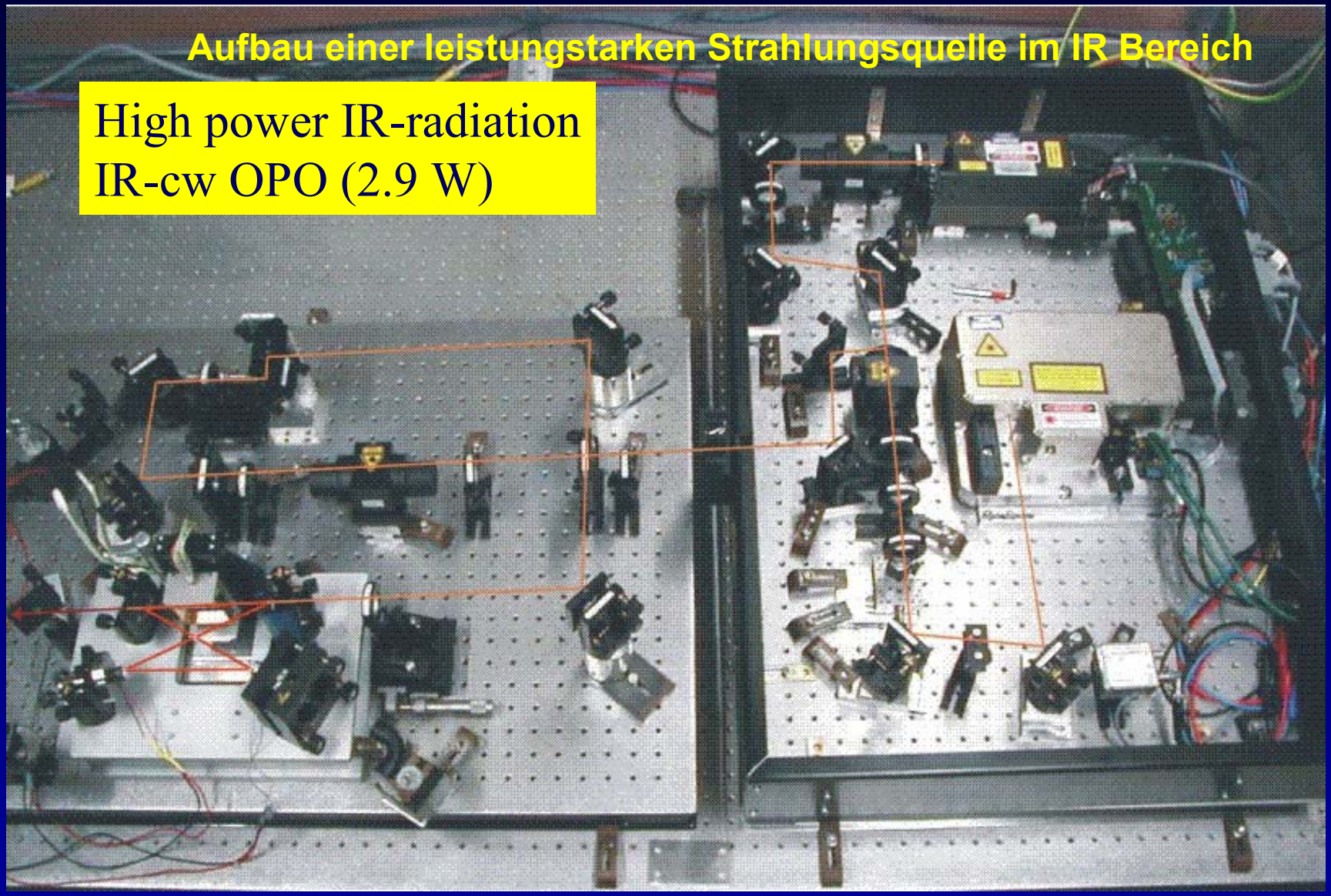

Pump laser: **M**aster **O**scillator **P**ower **A**mplifier: output power: 20 W at 1064 nm
Periodically **P**oled **L**ithium **N**iobate (quasiphase matched) **cw IR radiation 2.9 W**
resonant for signal wavelength (1485-1.665 nm) ; idler (3000-4000 nm)